JGR Solid Earth

RESEARCH ARTICLE
10.1029/2022JB024800

Geophysical-Petrological Model for Bidirectional Mantle Delamination of the Adria Microplate Beneath the Northern Apennines and Dinarides Orogenic Systems

Wentao Zhang[1,2], Ivone Jiménez-Munt[1], Montserrat Torne[1], Jaume Vergés[1], Estefanía Bravo-Gutiérrez[1], Ana M. Negredo[3,4], Eugenio Carminati[5], Daniel García-Castellanos[1], and Manel Fernàndez[1]

[1]Geosciences Barcelona, Geo3BCN-CSIC, Barcelona, Spain, [2]Department of Earth and Ocean Dynamics, University of Barcelona, Barcelona, Spain, [3]Departamento de Física de la Tierra y Astrofísica, Universidad Complutense de Madrid, Madrid, Spain, [4]Instituto de Geociencias, IGEO-(CSIC, UCM), Madrid, Spain, [5]Dipartimento di Scienze della Terra, Sapienza Università di Roma, Roma, Italy

Key Points:

- A new thermochemical structure of the crust and uppermost mantle is obtained along the northern Apennines, Dinarides, and Pannonian Basin
- The model distinguishes Adria and Tisza microplates with different crustal structures and lithosphere mantle compositions
- Two mantle wedges occur below the northern Apennines and Dinarides, resulting from the mantle delamination of Adria beneath its margins

Correspondence to:
I. Jiménez-Munt,
ivone@geo3bcn.csic.es

Citation:
Zhang, W., Jiménez-Munt, I., Torne, M., Vergés, J., Bravo-Gutiérrez, E., Negredo, A. M., et al. (2022). Geophysical-petrological model for bidirectional mantle delamination of the Adria microplate beneath the northern Apennines and Dinarides orogenic systems. *Journal of Geophysical Research: Solid Earth*, *127*, e2022JB024800. https://doi.org/10.1029/2022JB024800

Received 19 MAY 2022
Accepted 1 DEC 2022

Author Contributions:
Conceptualization: Ivone Jiménez-Munt, Montserrat Torne, Jaume Vergés, Manel Fernàndez
Formal analysis: Wentao Zhang, Estefanía Bravo-Gutiérrez
Funding acquisition: Ivone Jiménez-Munt, Daniel García-Castellanos
Investigation: Wentao Zhang, Ivone Jiménez-Munt, Montserrat Torne, Jaume Vergés, Ana M. Negredo
Methodology: Ivone Jiménez-Munt
Software: Ivone Jiménez-Munt

Abstract This study presents a geophysical-geochemical integrated model of the thermochemical structure of the lithosphere and uppermost mantle along a transect from the Northern Tyrrhenian Sea to the Pannonian Basin, crossing the northern Apennines, the Adriatic Sea, and the Dinarides fold-thrust belt. The objectives are to image crustal thickness variations and characterize the different mantle domains. In addition, we evaluate the topographic response of opposed subductions along this transect and discuss their implications in the evolution of the region. Results show a more complex structure and slightly higher average crustal density of Adria compared to Tisza microplate. Below the Tyrrhenian Sea and Western Apennines, Moho lays at <25 km depth while along the Eastern Apennines it is as deep as 55 km. The modeled lithosphere-asthenosphere boundary (LAB) below the Tyrrhenian Sea and Pannonian Basin is flat lying at ∼75 and 90 km, respectively. Below the External Apennines and Dinarides the LAB deepens to 150 km, slightly shallowing toward the Adriatic foreland basin at 125 km depth. Our results are consistent with the presence of two mantle wedges, resulting from the rollback of the Ligurian-Tethys and Vardar-NeoTethys oceanic slabs followed by continental mantle delamination of the eastern and western distal margins of Adria. These two opposed slabs beneath the Apennines and Dinarides are modeled as two thermal sublithospheric anomalies of −200°C. Most of the elevation along the profile is under thermal isostasy and departures can be explained by regional isostasy with an elastic thickness between 10 and 20 km.

Plain Language Summary This study integrates a wide range of geological and geophysical observations (e.g., elevation, gravity, geoid, seismic tomography) to investigate the density and temperature variations down to 400 km along a transect that extends from the Tyrrhenian Sea and northern Apennines in Italy to the Dinarides and Pannonian Basin in southern Europe. The main objectives are to study the present-day structure and composition of the lithosphere and uppermost mantle, and to evaluate the resulting topography, and finally to discuss their implications in the tectonic evolution of the region. Our results show that the crust and the base of the lithosphere vary significantly in the study region, lying shallow below the basins to much deeper underneath the mountain belts where topography is higher. We also observe two cold and dense zones sitting in the distal margins of the Adria microplate, beneath the northern Apennines and Dinarides, that are interpreted as two opposed subducting slabs that have largely controlled the geodynamic evolution of the study region in the last 30 My.

1. Introduction

The N-S convergence between the African and Eurasian plates since the Late Cretaceous is recognized as the primary causal mechanism for the squeezing of intervening microplates, bounded by narrow branches of the Neo-Tethys Ocean (e.g., Dewey et al., 1989). In particular, it drove to the development of subduction and collision orogens in the Central-Western Mediterranean region, which is a part of the active Alpine-Mediterranean mobile belt. The Adria microplate plays a key role in this geodynamic puzzle since Jurassic times, when the Vardar ophiolitic obduction started, followed by continental collisions with the Tisza microplate and Eurasian plate (Schmid et al., 2020). Subsequently, the NW-SE trending Dinarides orogenic belt developed along the NE margin of Adria whereas the NW-SE trending Apennines fold-thrust belt evolved in its SW margin. The Adria-Eurasia

Supervision: Ivone Jiménez-Munt, Montserrat Torne
Writing – original draft: Wentao Zhang
Writing – review & editing: Ivone Jiménez-Munt, Montserrat Torne, Jaume Vergés, Estefanía Bravo-Gutiérrez, Ana M. Negredo, Eugenio Carminati, Daniel García-Castellanos, Manel Fernàndez

convergence also produced the almost 1,000 km long ENE-WSW trending Alps orogenic belt (Figure 1) (e.g., Dewey et al., 1989; Handy et al., 2010; Stampfli & Borel, 2002).

The Western-Central Mediterranean region is a challenging area characterized by structural heterogeneity and tectonic complexity (e.g., Carminati et al., 2020; van Hinsbergen et al., 2020). The region has experienced a wide diversity of geodynamic processes, which include pre-orogenic rifting and oceanization, subduction and extinction of the Tethys oceanic lithosphere, counterclockwise rotation of the Adria microplate, back-arc spreading of the Tyrrhenian Sea and Pannonian Basin, and final continental collision and rapid uplift in the Apennines, Dinarides, Alps, and Carpathians (e.g., Carminati et al., 2012, 2020; Handy et al., 2015; Schmid et al., 2020; van Hinsbergen et al., 2019, 2020). All these deep geodynamic processes have a direct effect on the topography of the orogenic belts, producing the so-called dynamic topography (e.g., Faccenna et al., 2014; Kumar et al., 2021).

The structure and evolution of the Adria microplate is clearly described after decades of careful studies of its geology and geophysics. These studies reconstructed its crustal orogenic fold-belt structure and its upper mantle structure in three dimensions, interpreted as the result of subducted lithospheric slabs displaying abrupt changes in subduction polarity across transfer fault zones (e.g., Rosenbaum et al., 2008; Vignaroli et al., 2008). However, despite the wealth of data and research published about the study region (e.g., Artemieva & Thybo, 2013; Carminati & Doglioni, 2012; Kapuralić et al., 2019; Kästle et al., 2020), the current crustal and lithospheric structure and the topographic implications of the lithospheric anomalies are still under debate. Results on Moho depth show differences between deep seismic refraction profiles and receiver function (RF) results (Barchi et al., 2006; Finetti et al., 2001; Piana Agostinetti and Faccenna. 2018). Moreover, some tomographic models suggest that the Adriatic slab beneath the Apennines may be found nearby the mantle transition zone at ~300–400 km depth (e.g., Giacomuzzi et al., 2011; Hua et al., 2017; Zhao et al., 2016), while others suggest that the slab terminates at much shallower depths (~250 km; e.g., Lippitsch et al., 2003). Additionally, there are also discrepancies on the lithosphere-asthenosphere boundary (LAB) between seismic anisotropy models (Plomerová & Babuška, 2010), RFs (Belinić et al., 2018), thermal isostasy analyses (Artemieva, 2019) and on the origin of the highly variable topography. Recently, numerous geophysical surveys have investigated into the lesser-known composition and structure of the lithospheric mantle (e.g., Belinić et al., 2021; Blom et al., 2020; El-Sharkawy et al., 2020; Kästle et al., 2020). The surveys have elucidated the geometry of subducted slabs beneath the northern Apennines and Dinarides although the results vary significantly depending on the methodology used.

The prerequisite for a good understanding of the geodynamic evolution of the Western-Central Mediterranean region is to reconcile the observations obtained from different data sets and methods. The main aim of this study is to derive the present-day crust and upper mantle structure (down to 400 km depth) along a ~1,000 km transect, crossing in a SW-NE direction the Tyrrhenian Sea, the northern Apennines, the Adriatic Sea, the Dinarides and the Pannonian Basin (Figure 2a). The transect is sufficiently far from the potential influence of the subducted Alpine slab to allow straightforward interpretation of mantle seismic anomalies in terms of Apennines and Dinarides slabs. To determine the lithospheric structure along the transect we applied an integrated geophysical-petrological modeling tool, which combines surface heat flow (SHF), Bouguer anomaly, geoid height, elevation and petrological data to produce the thermal, density, and seismic velocity structure of the crust and upper mantle as described in Kumar et al. (2020). A similar approach has been used to study the deep structure of the Gibraltar Arc region (Jiménez-Munt et al., 2019) and along the Algerian and Alboran basins of the Western Mediterranean (Kumar et al., 2021). Both studies demonstrated that the pull force of hanging lithospheric slabs is markedly different if the slab is still attached to the continental lithosphere or is detached after break-off processes. They also permitted to determine the up-down direction, amount and extent of the dynamic topography linked to the sub-lithospheric forces as well as its impact at the surface.

The crustal and lithospheric structures obtained in this study are compared with previous interpretations and discussed in terms of the geodynamic evolution of studied tectonic domains within the complex and long-term evolving Alpine-Mediterranean mobile belt. Lastly, the contribution of deep geodynamic processes in the build-up of present orogenic topographic relief is discussed.

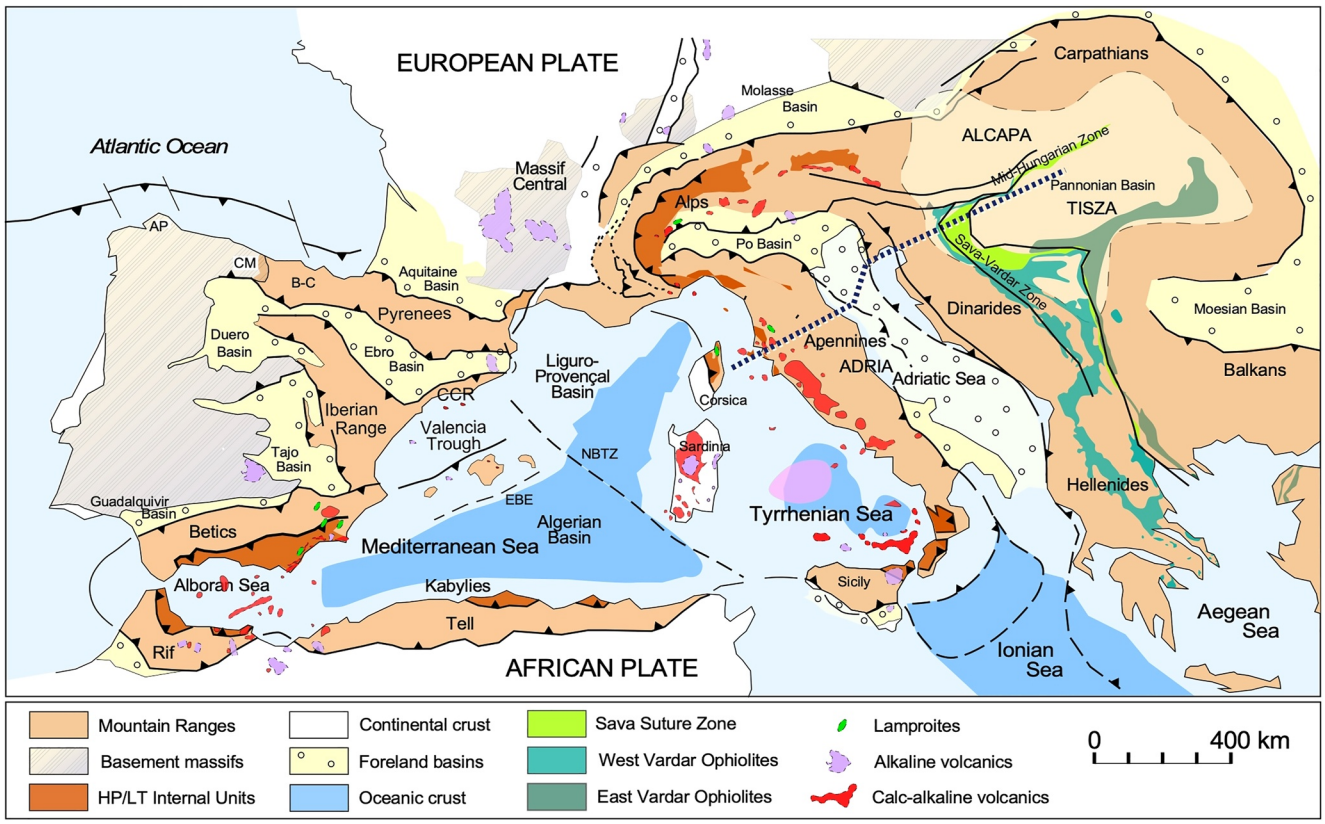

Figure 1. Tectonic map of the Western-Central Mediterranean region with the main orogenic belts and foreland basins.

2. Geological Setting

The Western-Central Alpine Mediterranean orogenic system is the result of the interplay between Eurasian plate and the Adria and Tisza microplates (originally separated by Vardar oceanic domain, a northern branch of the Neo-Tethys) in the framework of the Africa-Eurasia convergence. At upper crustal levels, the main tectonic domains that evolved on the Adria microplate are, from west to east, the NE-directed Apennines and the SW-directed Dinarides orogens with their common foreland basin along the entire Adriatic Sea. The Apennines mainly developed during the W- to SW-dipping subduction of the Alpine Tethys oceanic domain (that separated Adria microplate from Eurasian plate) and the following subduction of the Adria thinned margin (Doglioni, 1991; Faccenna et al., 2001; Molli, 2008), that drove to the deformation of cover rocks of the SW margin of Adria. The eastward retreat of the subducting-plate hinge generated the ENE-directed Apennines orogenic system and the development of a complex back-arc basin system (e.g., Doglioni et al., 1997; Lacombe & Jolivet, 2005; Le Breton et al., 2017; Malinverno & Ryan, 1986; Patacca et al., 1990; Romagny et al., 2020; Royden, 1993). The Corsica-Sardinia lithosphere was drifted from the southern Europe continental margin (Doglioni et al., 1997; Romagny et al., 2020), and it is located between the Liguro-Provencal and Tyrrhenian back-arc basins. The Dinarides lie along the deformed NE margin of Adria and have a longer and more complex history that includes subduction of the Vardar Ocean basin. This long-term subduction produced a first late Jurassic obduction of oceanic lithosphere and a later continental collision between Adria and Tisza microplates (Channell et al., 1996; Schmid et al., 2020), presently forming the thinned crust flooring the northern region of the Pannonian Basin along the easternmost segment of the transect. The Tisza crustal domain is welded to the Eurasian plate (Figure 1).

The Apennines orogenic system is characterized by two tectonic domains; the Internal (western) Apennines including the Ligurian-Tuscan-Tyrrhenian regions toward the WSW and the External (eastern) Apennines comprising the Apennines fold-thrust belt and the Adriatic foreland basin toward the ENE (e.g., Barchi et al., 1998, 2003; Cosentino et al., 2010; Molli, 2008; Scrocca, 2006). Evidence for oceanic and continental subduction is provided by metaophiolites and metasedimentary rocks of the Adria passive margin with late Cenozoic HP-LT metamorphism

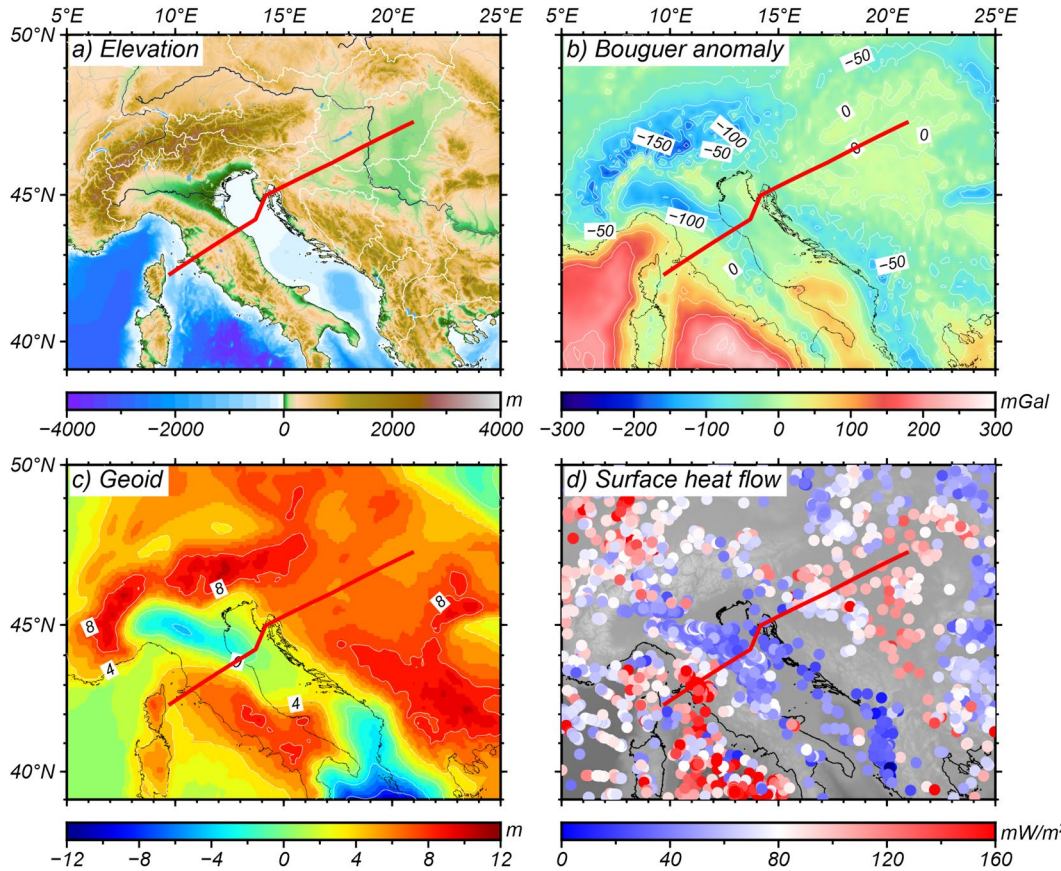

Figure 2. (a) Elevation data come from topo_19.1.img (Smith & Sandwell, 1997, updated 2019). Major flat areas characterized the Pannonian Basin and the northern Adriatic Sea, which contrasts with the relief of the Dinarides and Apennines mountain belts. (b) Bouguer gravity anomaly has been obtained applying the complete Bouguer correction to the free air gravity anomaly data (Sandwell et al., 2014, updated 2019) using the software FA2BOUG (Fullea et al., 2008) with a density reduction of 2,670 kg/m^3. Areas with high relief show gravity lows, while the basins are characterized by relative gravity highs. Note that most of the Pannonian Basin has near-zero Bouguer gravity values. A strongest positive Bouguer anomaly of 200–300 mGal marks the abyssal areas of the Tyrrhenian sea, whereas the Adriatic Sea show values between 0 and 60 mGal. (c) Geoid height data were derived from the global gravitational model GECO (Gilardoni et al., 2016), filtered up to degree and order 10. For most of the region, the geoid shows positive values, except for the Po plain and southern Adriatic Sea. The Alps, Apennines and southern Dinarides are characterized by relative highs (locally up to 10 m). (d) Surface heat flow data from the Global Heat Flow Database (Fuchs & Norden, 2021) and completed with the Italian National Geothermal Database (Pauselli et al., 2019; Trumpy & Manzella, 2017). Highest values above 120 mW/m^2 are observed in the Tyrrhenian Sea and Tuscan domain while the Adriatic Sea and Dinarides record lower values (40–50 mW/m^2). In the Pannonian Basin, average heat flow ranges from 80 to 100 mW/m^2.

cropping out in the northern Tyrrhenian islands and in the Tuscan region (Bianco et al., 2015; Rossetti et al., 1999; Vignaroli et al., 2009). The Northern Tyrrhenian Basin as well as the Ligurian-Tuscan domains are characterized by thin stretched continental crust (e.g., Jolivet et al., 1998; Moeller et al., 2013, 2014; Sartori et al., 2004) modified by extensive volcanism and intruded by large magmatic bodies (e.g., Dini et al., 2005; Rocchi et al., 2010; Serri et al., 1993). This igneous activity features a large range of compositions, from subalkaline to ultra-alkaline and from ultrabasic to acid (Lustrino et al., 2022). The Tyrrhenian Basin began to open during the Tortonian (e.g., Keller & Coward, 1996; Keller et al., 1994; Sartori et al., 2004; Trincardi & Zitellini, 1987), and extension overprinted and partially re-used the compressional structures, as observed also in the axial/eastern sector of the Apennines fold-thrust belt (e.g., Barchi et al., 2021; Bonini & Sani, 2002; Collettini & Barchi, 2002; Curzi et al., 2020; Keller et al., 1994).

The Apennines fold-thrust belt and its undeformed foreland display a complex ENE-directed system of thrust imbricate structures, involving mainly thin-skinned and possibly thick-skinned structural styles (e.g., Bally, 1987; Barchi et al., 1998; Conti et al., 2020; Coward et al., 1999; Massoli et al., 2006; Mazzoli et al., 2005; Molli

et al., 2010; Mostardini & Merlini, 1986; Patacca et al., 1990). Compression migrated from the Tyrrhenian area toward the Adriatic foreland from Oligocene to Pliocene-Pleistocene (Doglioni et al., 1996; Keller & Coward, 1996; Noguera & Rea, 2000; Patacca & Scandone, 2001, 2007), whereas coeval extension collapsed the Internal Apennines (Cavinato & DeCelles, 1999; Patacca et al., 1990). The analysis of syn-orogenic and thrust-top deposits allowed the recognition of ∼100 and ∼200 km progressive eastward migration of the thrust fronts in the last 25 My in the northern and central Apennines, respectively (Boccaletti et al., 1990; Vezzani et al., 2010). The Adriatic Sea, the shared foreland of southern Alps, Apennines, and Dinarides, shows variable tectonic style and age along strike (Cuffaro et al., 2010; Fantoni & Franciosi, 2010; Ghielmi et al., 2010; Scrocca, 2006; Tinterri & Lipparini, 2013; Wrigley et al., 2015) that are controlled by superimposition of pre-shortening (Jurassic rift-related) inherited structures of Adria microplate (Wrigley et al., 2015), and the Apennines and Dinarides orogenic imprint through time (Balling et al., 2021). The well-constrained northern Apennines frontal thrust system displays 45 km of shortening in the last 17 My at shortening rates of 2.9 mm/yr (Basili & Barba, 2007), with slip rates for different thrusts in the 0.26–1.35 mm/yr range (Maesano et al., 2013).

The WSW-directed Dinarides orogenic system is built by multiple orogenic processes related to the progressive closure of the Vardar Ocean since Late Jurassic time (e.g., Channell et al., 1996; Chiari et al., 2011; Gallhofer et al., 2017; Maffione and van Hinsbergen, 2018). The first of these large-scale plate tectonic processes was the obduction of the Western Vardar Ophiolite Unit on top of the NE Dinarides with a total displacement of ∼180 km. The end of the Vardar oceanic subduction led to the continental collision between Adria (lower plate) and Eurasian (upper plate) along the Sava Suture Zone (Handy et al., 2015; Pamić et al., 1998; Schmid et al., 2008, 2020; Ustaszewski et al., 2010).

The northern and central Dinarides fold-thrust belt is divided into the Internal Dinarides in the east, directly in contact with the Sava Suture Zone, and the External Dinarides in the west (Placer et al., 2010; Schmid et al., 2004; Tari, 2002; Tomljenović et al., 2008). The Internal Dinarides consist of composite thrust sheets (Balling et al., 2021; Schmid et al., 2008, 2020), including obducted Western Vardar Ophiolites (Robertson et al., 2009) and Mesozoic cover rocks (platform carbonates and foredeep deposits) belonging to the NE distal margin of Adria (Tari, 2002; Tomljenović et al., 2008). The External Dinarides are characterized by thrust imbricates of sedimentary cover units, locally involving Paleozoic basement, belonging to the NE margin of the Adria microplate shortened from the Eocene to the Present, although shortening was interrupted by a period of extension in Miocene time (e.g., Schmid et al., 2008; Tari, 2002; Van Unen et al., 2019). Shortening propagated in-sequence from the Sava Suture Zone in the east to the Adriatic foreland in the west (Ustaszewski et al., 2010). Total shortening increases from 50 to 130 km toward the south of Dinarides (Schmid et al., 2020 and references therein; Balling et al., 2021), although these estimates can vary significantly owing to different paleogeographic reconstructions (Korbar, 2009; Pamić et al., 2002). The internal parts of the Dinarides are characterized by abundant Paleogene-middle Miocene calcalkaline to ultrapotassic magmatism, (e.g., Kovács et al., 2007, and references therein).

The Pannonian Basin, to the NE of the Sava Suture Zone, is surrounded by the Alpine, Carpathians and Dinarides orogenic belts and is a Miocene to Present extensional back-arc basin underlain by thinned continental lithosphere (e.g., Horváth, 1995; Horváth et al., 2006; Koroknai et al., 2020). The substratum of the Pannonian Basin is made up by two megatectonic units: the Alpine-Carpathian-Pannonian (AlCaPa) and the Tisza, separated by the WNW-ENE Mid-Hungarian Shear Zone (Csontos & Nagymarosy, 1998; Schmid et al., 2008; Hetényi et al., 2015). The indentation of the Adria microplate during the Pliocene-Quaternary triggered mild compression through the Pannonian Basin (Bada et al., 2007; Horváth et al., 2006; Matenco & Radivojević, 2012). The Pannonian Basin hosts Miocene to recent magmatic rocks with diverse compositions (calc-alkaline, K-alkalic, ultrapotassic and Na-alkalic; Seghedi & Downes, 2011).

3. Methods

Modeling of the thermal lithosphere, hereinafter referred to as lithosphere, along the study transect was performed using LitMod2D_2.0 (Kumar et al., 2020), an updated version of the original 2D software developed by Afonso et al. (2008). Assuming thermal isostasy, thermal steady state and a planar approximation (Cartesian coordinates), the algorithm integrates petrological and geophysical data to study the 2D thermo-chemical structure and the seismic velocity distribution of crust and upper mantle, fitting simultaneously absolute elevation, geoid height, Bouguer gravity anomalies, and SHF (Figure 2).

Table 1
Thermo-Physical Properties of the Crustal Tectonic Units Along the Profile

Crustal domains		Density (kg/m^3)	Thermal conductivity (W/K m)	Radiogenic heat production (μW/m^3)
Adria microplate	Sediment	2,450	2.4	1
	Elba granits	2,750	3.1	3.5
	Apennines UC/Tuscany MP	2,750–2,800 (a)	2.7/3.1	1.3/3.8
	Apennines MC/Tuscany MP	2,820	2.7/3.1	0.8/3.0
	Apennines LC/Tuscany MP	2,920	2.1/3.1	0.6/1.0
	Dinarides MC	2,850	2.7	0.8
	Dinarides LC	2,920	2.1	0.6
	Apennines/Dinarides duplicated LC	2,950	2.1	0.6
Tisza microplate	Sava Suture	2,850	2.7	1.3
	Pannonian Basin UC	2,750–2,860 (a)	2.9	2
	Pannonian Basin LC	2,950	2.1	0.6

Note. UC: Upper crust; MP: Magmatic Province; MC: Middle Crust; LC: Lower Crust. (a) Calculated as a function of pressure.

The numerical domain extends from the surface to 400 km depth. It is defined by different crustal and mantle bodies characterized by their individual thermo-physical properties and chemical composition. Crustal bodies are described by the user using thermo-physical properties (e.g., Table 1, thermal conductivity, volumetric heat production rate, density, coefficient of thermal expansion and compressibility), with an option of depth and/or temperature dependence. The composition of upper mantle bodies is defined using the Na_2O–CaO–FeO–MgO–Al_2O_3–SiO_2 (NCFMAS) system (Table 2). The Gibbs free-energy minimization algorithm (Connolly, 2005, 2009) is used to compute stable phases and mineral assemblages within the temperature and pressure ranges of the upper mantle. The density distribution is obtained with an iterative scheme to include the effect of pressure, temperature, and composition. Mantle thermal conductivity is also P-T dependent.

Temperature distribution within the lithosphere is calculated by solving the 2D steady-state heat conduction equation. where boundary conditions are set as two fixed isotherms, that is, 0°C at the surface and 1,320°C at the LAB. Below the LAB, LitMod2D_2.0 considers a 40-km thick thermal buffer with a temperature of 1,400°C at its base to avoid unrealistic discontinuities between the conductive thermal gradient within the lithosphere and the sublithospheric adiabatic thermal gradient.

Table 2
Major Oxides Composition in % of Weight Percent in the NCFMAS System Used for the Lithospheric and Sublithospheric Mantle

	Sublithospheric mantle	Mantle wedge	Lithospheric mantle	
Composition	DMM (Workman & Hart, 2005)	DMM—3% (Kumar et al., 2021)	Adriatic mantle (Tc_2) Av. Tecton peridotite (Griffin et al., 2009)	Pannonian mantle (PB_mant) (Alasonati Tašárová et al., 2016; Downes et al., 1992)
SiO_2	44.7	44.59	45	44.6
Al_2O_3	3.98	3.51	3.9	2.9
FeO	8.18	8.21	8.1	8.8
MgO	38.73	39.63	38.7	40.8
CaO	3.17	3.02	3.2	2.6
Na_2O	0.13	0.082	0.28	0.18
Mg# (100 * MgO/[MgO + FeO])	89.4	89.58	89.5	90.4

Note. DMM, Depleted Mid-Oceanic Ridge Mantle; Tc_2, Average Phanerozoic Mantle; PB_mant, Pannonian Basin mantle.

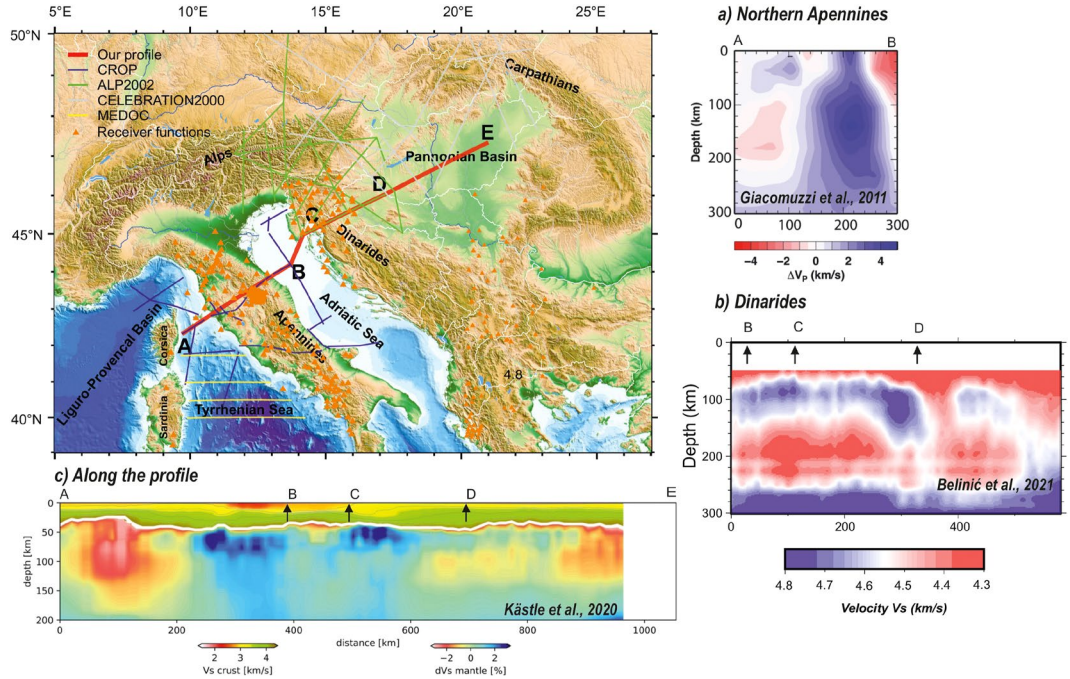

Figure 3. Upper mantle characterization from previous studies. (a) P-wave teleseismic tomography from Giacomuzzi et al. (2011). (b) Shear-wave velocity structure beneath the Dinarides from the inversion of Rayleigh-wave dispersion after Belinić et al. (2021) that have been used to constrain the SCLM anomaly below the Dinarides (Figure 5f). (c) Crustal S-wave velocity, Moho depth (white line) and mantle V_s anomaly from Kästle et al. (2020) model along our profile.

The final density distribution is used to calculate elevation, Bouguer and free air gravity anomalies, and geoid height. Seismic velocities are calculated based on phase and mineral assemblages and on the obtained temperature and pressure conditions and are compared with available velocity and tomography models. LitMod2D approach has been successfully applied in different tectonic settings including continental margins (e.g., Fernàndez et al., 2010; Pedreira et al., 2015) and continental collisional regions (e.g., Carballo et al., 2015; Jiménez-Munt et al., 2019; Kumar et al., 2021; Tunini et al., 2015). For more details about LitMod2D the reader is referred to Afonso et al. (2008) and Kumar et al. (2020).

Moho depth and crustal geometry are mainly constrained by available active and passive seismic experiments (DSS and RFs) and geological cross-sections, as discussed in the following section. The chemical composition of the mantle is obtained from xenoliths data when available, or according to its tectonothermal age as explained in Griffin et al. (2009). The LAB depth and the composition of the mantle (i.e., lateral compositional domains) are subsequently refined based on the fitting of the geophysical observables: elevation, gravity anomaly, geoid high, SHF and mantle seismic velocities (Figure 3; e.g., Belinić et al., 2021; Giacomuzzi et al., 2011; Kästle et al., 2018; Koulakov et al., 2015).

4. Lithospheric Structure and Upper Mantle Characterization From Previous Studies

4.1. Crustal Structure

During the last three decades, a large amount of geologic and geophysical investigation has been carried out to image the crustal structure of the study region. Along the transect, geophysical data come from deep near-vertical reflection (e.g., Scrocca et al., 2003) and wide-angle reflection/refraction seismic experiments (e.g., Cassinis et al., 2005), RF analyses (e.g., Mele & Sandvol, 2003) and gravity modeling (e.g., Šumanovac, 2010). Additional data come from seismicity distribution at crustal and subcrustal levels (e.g., Chiarabba et al., 2004; De Luca et al., 2009). These studies show that shallow seismicity is mainly concentrated along a narrow band along the backbone of the Apennines while a diffuse activity characterizes the Adriatic region. At crustal levels, focal mechanisms evidence normal faulting below the central part of the Apennines belt and thrust/reverse faulting mechanisms at the outer fronts of the Apennines (e.g., Chiarabba et al., 2014; De Luca et al., 2009). Seismicity

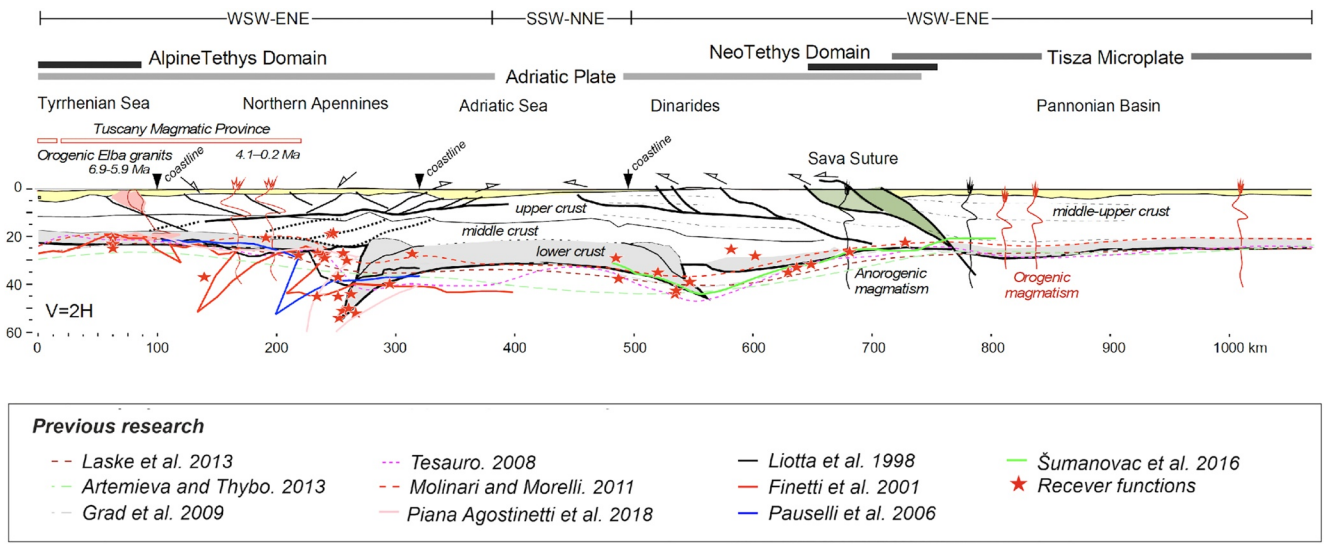

Figure 4. Crustal structure from the best fitting model constrained from the available geological and geophysical information listed in the text and in the panel legend. Yellow color is the sediment layer. Moho depths from previous studies and receiver functions (Chiarabba et al., 2014; Diaferia et al., 2019; Mele & Sandvol, 2003; Piana Agostinetti & Amato, 2009; Piana Agostinetti & Faccenna, 2018; Stipčević et al., 2020; Šumanovac et al., 2016) are shown for comparison.

between 25 and 70 km is widespread in the Adriatic region with a tendency to cluster below the Apennines while no deep earthquakes were recorded below the Tyrrhenian Sea (Figures 8 profile E–F of De Luca et al., 2009). The west dipping seismicity, registered down to 70 km depth, is interpreted as the evidence of the subduction of the Adriatic lithosphere beneath the Apennines (De Luca et al., 2009). In the Tyrrhenian basin, the crustal structure is constrained by the CROP line M-12A, while the onshore CROP 03 was used to constrain the crustal geometry of the Apennines and the western region of the Adriatic Sea (Barchi et al., 1998; Finetti et al., 2001; Liotta et al., 1998; Pauselli et al., 2006; Piana Agostinetti & Faccenna, 2018). In the Adriatic Sea we used the CROP M-16 seismic line. For the Dinarides and the western Pannonian Basin, we used the Alp07 profile (Šumanovac et al., 2016) and the earthquake tomography analysis of Kapuralić et al. (2019). In addition to these profiles, we have projected onto the transect the Moho depth data from EUNAseis (Artemieva & Thybo, 2013), CRUST1.0 (Laske et al., 2013) and EPcrust (Molinari & Morelli, 2011) models and the high-resolution Eurasian Moho data set of Tesauro et al. (2008) and Grad et al. (2009). For the Dinarides and Pannonian Basin additional information comes from seismicity distribution (e.g., Kuk et al., 2000 and Bondár et al., 2018, respectively).

There is agreement on the broad features of the crustal structure; however, important discrepancies arise when entering into the details of its internal structure and density distribution. All studies agree that the Moho lies at shallow depths (20–25 km) in the Tyrrhenian Sea and below western Italy, at intermediate depth (30–35 km) along the Adriatic coast, deepening under the Apennines (down to 50 km) and Dinarides (down to 45 km) mountain belts (Figure 3; e.g., Kapuralić et al., 2019; Molinari et al., 2015; Stipčević et al., 2020). In the Apennines, the complex internal crustal structure, the possible presence of a mantle wedge and the top of the subducting slab is reflected in the RFs results where differences in the Moho depth may be as large as 30 km from one study to another (Chiarabba et al., 2014; Mele & Sandvol, 2003; Piana Agostinetti & Faccenna, 2018). Major discrepancies are also observed in the interpretations of multichannel seismic reflection profiles about the internal structure of the crust and the exact location and geometry of the top of the subducting slab (Figure 4). Finetti et al. (2001), based on the interpretation of onshore CROP-03 profile, favor a complex thrust system with thrust faults and shear planes that extend at low angle from the crust to the upper mantle offsetting the Moho. These authors also favor a westward location of the top of the subducting slab, compared to the location proposed by Pauselli et al. (2006) and Piana Agostinetti and Faccenna (2018) who place it right below the External Apennines (Figure 4). This latter interpretation is more in line with RFs and seismicity results of Mele and Sandvol (2003) and Chiarabba et al. (2014, 2020). Receiver functions and seismic tomography indicate that beneath the Internal Apennines the shallowest mantle is characterized by about 5% lower shear wave velocity anomaly and 3% higher V_p/V_s ratio than the reference values for these depths (Chiarabba et al., 2020). These authors interpreted these anomalies as mantle upwelling with the presence of melts at the base of the crust, extending from the

Tyrrhenian to the central Apennines. Below the Dinarides, Kapuralić et al. (2019) using local earthquake tomography inferred Moho depths between 40 and 45 km, similar to those obtained by Šumanovac et al. (2016) using RFs. A quite flat Moho around 25 km depth is observed underneath the back-arc Pannonian Basin (Kapuralić et al., 2019; Šumanovac et al., 2016). From local earthquake tomography, Kapuralić et al. (2019) found high velocities below the northern Dinarides at depths shallower than 10 km, but low velocities in the Pannonian Basin associated with a deep local depression. They also imaged a high-velocity body at 5–15 km depth between the Dinarides and the Pannonian Basin. The Dinaridic crust has been interpreted as two-layered, while the Pannonian crust is interpreted as single-layered (Kapuralić et al., 2019; Šumanovac et al., 2016).

4.2. LAB and Upper Mantle Characterization

In the study area a number of RF studies have focused on the LAB (Belinić et al., 2018; Geissler et al., 2010; Miller & Piana Agostinetti, 2012). Tomography, mainly based on teleseismic body-wave (e.g., Koulakov et al., 2009; Lippitsch et al., 2003; Piromallo & Morelli, 2003), P and surface wave tomography (e.g., Belinić et al., 2021; El-Sharkawy et al., 2020; Giacomuzzi et al., 2011; Kästle et al., 2022) and full-wave inversion of body and surface waves (e.g., Beller et al., 2018; Blom et al., 2020; Zhu et al., 2015) have provided images of the upper mantle down to the transition zone. All of them show strong lateral heterogeneities, where the different depths of the discontinuities, and the various shapes and lengths of the imaged slabs highlight the complexity of the region. Although comparison of tomography images is not forthright because mismatch in the location of the anomalies may be partly due to the different methods and sensitivities of the modeled wave types, the 3D structural complexity of the region adds a degree of uncertainty that is reflected in the variety of models proposed so far.

Comparison of available seismic LAB depths shows a high degree of variability between the main tectonic domains. Below the northern Apennines, Miller and Piana Agostinetti (2012), based on S-RFs, highlighted a complex lithospheric structure with two different S-velocity jumps, located at ∼90 and 180 km depth. The shallowest one is interpreted as the LAB of the upper plate while the deepest jump is proposed to be associated with the LAB of the subducting lithosphere. This interpretation in terms of subducted/delaminated Adriatic lithosphere below the Apennines agrees with the location and distribution of the west-dipping seismicity down to about 70 km (e.g., Chiarabba et al., 2005; De Luca et al., 2009). Underneath the Dinarides discrepancies of the seismic LAB may reach up to 20 km, from 120 to 100 km depth, shallowing up toward the Adriatic Sea (90 km depth) and Pannonian Basin, where the LAB is placed at a rather constant depth of 70 km (e.g., Belinić, et al., 2018). These studies also highlight the variability of the LAB depth encountered along the Dinarides, with deep LABs in the Northern and Southern regions (100–120 and 90 km depth, respectively) that contrast with the much shallower LAB (∼50 km depth) in the central Dinaric region (Belinić et al., 2018; Šumanovac et al., 2017).

As mentioned, tomography images differ substantially depending on the methods used. While global models (e.g., Amaru, 2007 or Zhu et al., 2015) are not conclusive due to their low resolution, regional and local models show a high variability with the presence of subducted slabs, attached slabs of variable lengths and detached slabs (Blom et al., 2020; El-Sharkawy et al., 2020). These studies, based on a high-resolution shear-wave velocity model, find the presence of slab segments in the northern Apennines, beneath the Dinarides and in the central Alps. Below the Apennines, Hua et al. (2017), based on P-wave anisotropic tomography, image a vertically oriented slab extending down to ∼300 km, a result that is coincident with that obtained by Benoit et al. (2011), who combined teleseismic P- and S-wave arrival time data. Studies based on P-wave teleseismic tomography find that the slab reaches depths of 400–500 km (Giacomuzzi et al., 2011) and 350–400 km (Hua et al., 2017; Spakman & Wortel, 2004). This result is coincident with that obtained by Koulakov et al. (2015), who, based on body-waves analysis, find a steeply dipping high-velocity anomaly down to 400 km, that they interpret as composed of the continental lithospheric mantle of Adria. Overall, these studies image shallower slab depths than previous models with less resolution (e.g., Lucente et al., 1999; Piromallo & Morelli, 2003), which predicted that the slab penetrates well into the transition zone.

Inversion of Rayleigh-wave dispersion by Belinić et al. (2021) shows a high-velocity anomaly reaching depths of 160 km beneath the northern Dinarides and more than 200 km beneath the southern regions. These results differ slightly from those obtained by Šumanovac and Dudjak (2016) and Šumanovac et al. (2017), who, based on teleseismic tomography, conclude that in the northern Dinarides the pronounced fast anomaly reaches 250 km depth. The observed NE dipping fast anomalies in the northern region extend underneath the entire Dinarides fold-thrust belt, indicating the sinking of cold and rigid material of the Adriatic microplate. Belinić et al. (2021)

imaged low velocity zones under the southwestern Pannonian Basin and beneath the central part of Adria, which they interpreted as results of lithospheric thinning and/or upwelling of hot asthenospheric material.

5. Results

Here, we summarize the main results of the crustal structure (Figure 4) and the physical properties of the lithospheric and sublithospheric mantle resulting from the best fit model (Figures 5 and 6). The obtained lithospheric model is defined by a series of crustal and mantle bodies, with the crustal physical parameters and the chemical composition of the mantle shown in Tables 1 and 2, respectively. The boundaries of the mantle domains shown in Figure 5f must be understood as transitional (with physical properties changing gradually) and not abrupt, as drawn for simplicity in the figure.

5.1. Crustal Structure

Figure 4 shows the modeled crustal structure, which has been constrained by available seismic data and geological-cross sections and slightly modified to match the surface observables, after modifying the geometry and composition of the less constrained mantle bodies. Modifications of the crustal structure are always within the uncertainties of available data. Crustal density values have been taken from previous gravity modeling (Šumanovac, 2010) and calculated by empirical velocity-density relationships (Brocher, 2005), considering the crustal velocity models (e.g., Kapuralić et al., 2019; Molinari et al., 2015). Thermal conductivities and radiogenic heat production come from previous studies (e.g., Norden & Förster, 2006; Trumpy & Manzella, 2017) and from the global compilation by Vilà et al. (2010). Moreover, we consider specific thermal parameters for the Tuscany region and Internal Apennines, where SHF (Figure 2) shows high values probably related to active hydrothermal flow and magmatism, as indicated by the presence of active hydrothermal systems and recent volcanic and magmatic activity (e.g., Pandeli et al., 2013; Sani et al., 2016). We modeled the high SHF within the Tuscany Magmatic Province by high conductivity and radiogenic heat production, which correlates with a crust with magmatic intrusions and the presence of granitoids (Norden & Förster, 2006), cropping out and reached by drill holes in the area (e.g., Dini et al., 2005). In contrast, lower heat flow values (<60 mW/m^2) are found in the Internal Apennines and Dinarides, whereas in the Pannonian Basin heat flow values are above 70 mW/m^2.

According to geological and geophysical information and the best fit of geophysical observables, we distinguish the Adriatic microplate, extending from the Tyrrhenian basin to the Dinarides, and the Tisza microplate, which in the modeled transect encompasses the western half of the Pannonian Basin. These two microplates are separated by the Sava Suture Zone (a remnant of the formerly intervening oceanic domain; Figures 4 and 5) and differ in their internal crustal structure and average densities.

The Moho lies at variable depths, deepening slightly from ~23 km under the Tyrrhenian basin to ~25 km under the Internal Apennines. The Moho depth in the External Apennines increases from ca. 35 km in the east to ca 52 km in the west. Beneath the Adriatic Sea, the Moho remains at a rather constant depth (>30 km) deepening underneath the External Dinarides, where it is locally found at 45 km. East of the Sava Suture Zone, the Tisza microplate shows very little crustal thickness variation, with values decreasing from 30 km in the west to 25 km in the easternmost part of the Pannonian Basin.

In our favored model, three crystalline layers (Figure 4) characterize the crust of the Adriatic microplate. Crustal densities range from 2,750 kg/m^3 for the upper crust, 2,820–2,850 kg/m^3 for the middle crust and 2,920–2,950 kg/m^3 for the lower crust. However, we cannot rule out a two-layered crust, with upper-middle and lower crust with an average density of 2,800 kg/m^3 for the upper-middle part. These crystalline layers are covered by a sedimentary layer of variable thickness with an average density of 2,450 kg/m^3. In terms of crustal average density, within the Adriatic microplate we can distinguish the Tuscany Magmatic Province with values ~2,780 kg/m^3 and the External Apennines, Adriatic Sea and Dinarides ~2,830 kg/m^3. The temperature at Moho depth is ~430°C in the Adriatic Sea, gradually increasing with the crustal deepening below the Apennines (~700°C) and the Dinarides (~500°C). The Tuscany Magmatic Province is characterized by high temperatures at shallow levels with values around 100°C at 2 km depth. The Moho temperature increases from 400°C in the western part of the profile in the Tyrrhenian Sea to 530°C in the Internal Apennines. These higher values in an area with thin crust are probably related to upwelling of hot sublithospheric material.

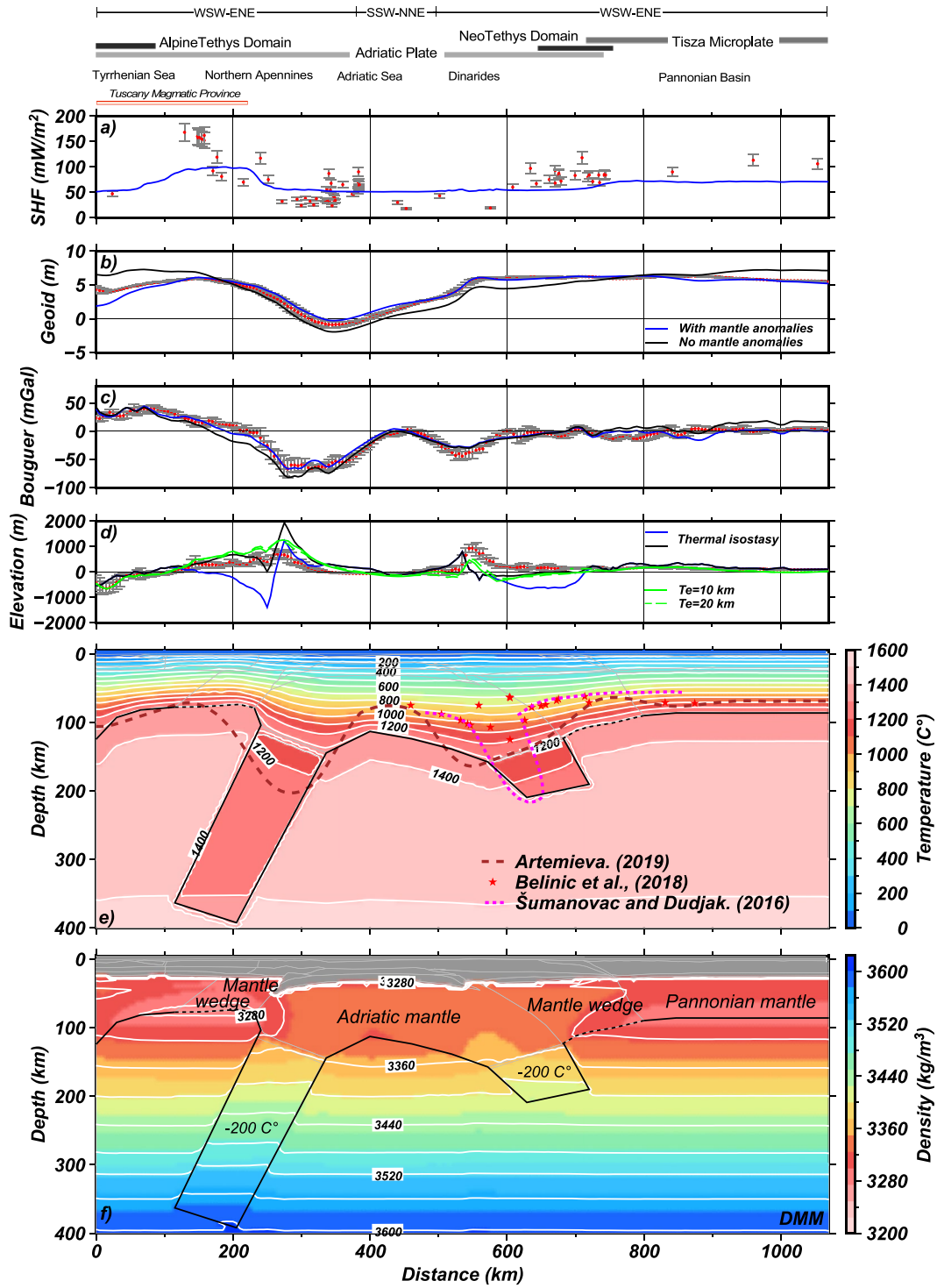

Figure 5. Best fit model. Surface observables (red dots): (a) Surface Heat flow, (b) Geoid height, (c) Bouguer anomaly and (d) absolute elevation, are projected onto the transect at 5 km sampling interval within a strip of 25 km half-width to account for lateral variations perpendicular to the strike. Standard deviations are shown as error bars. Blue and black lines show calculated values with and without sublithosphere anomalies, respectively. In (d) blue and black lines show thermal isostatic elevation (with and without mantle anomalies), and green lines are the calculated flexural elevation with elastic thickness Te = 10 km and dashed line Te = 20 km. Panel (e) shows the temperature distribution for the whole lithosphere. Panel (f) shows the density distribution within the lithospheric mantle along the modeled transect. See Figure 1 for location.

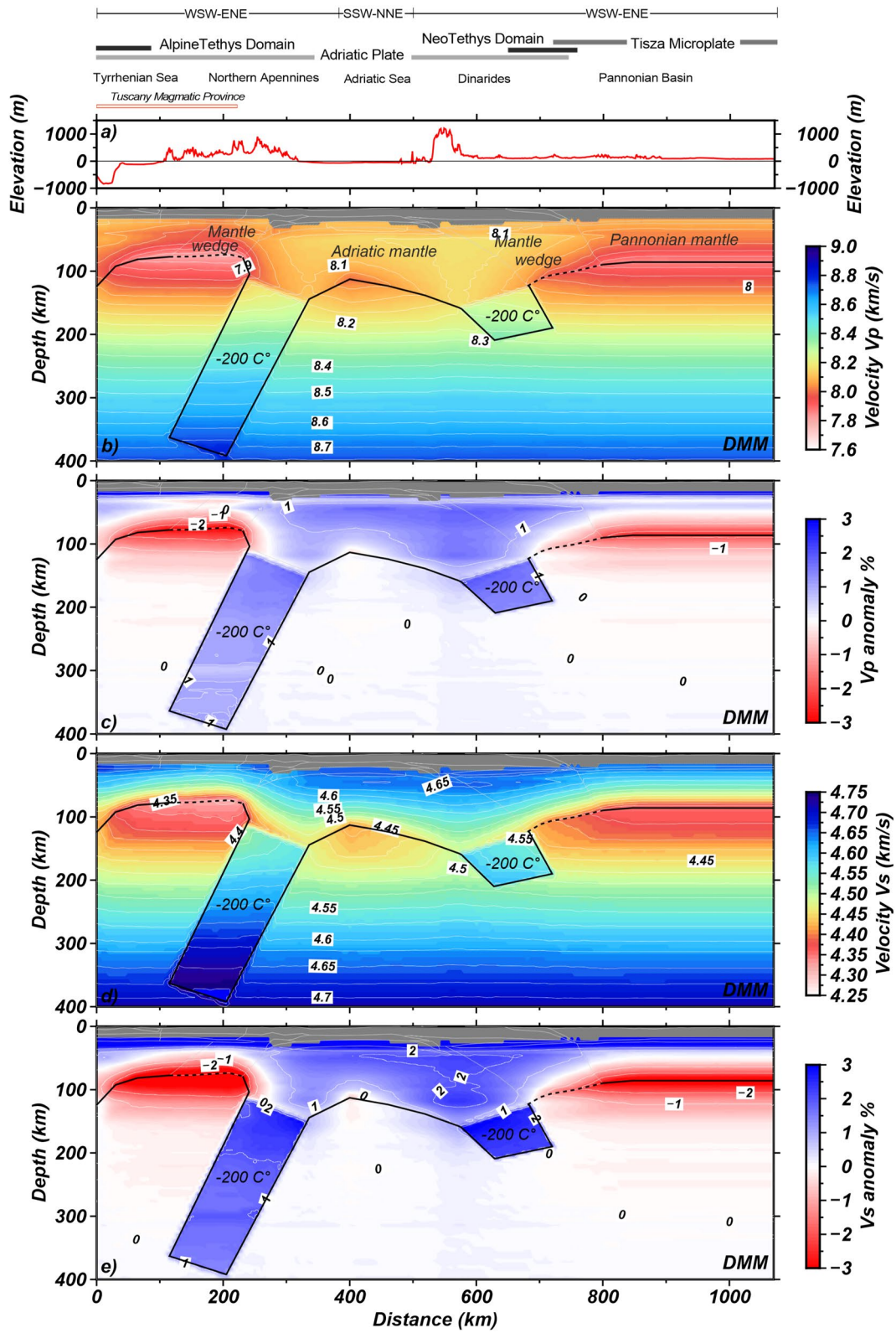

Figure 6. Mantle seismic velocities and synthetic seismic velocity anomaly along the transect. Panel (a) shows elevation profile, (b) and (d) show absolute P- and S-wave velocities and (c) and (d) synthetic P and S-wave anomalies, respectively.

The modeled crustal structure of the Pannonian Basin is characterized by a two-layer crystalline crust, covered by a 4–6 km thick sedimentary layer (Figure 4). The upper-middle crust with an average density of 2,750 kg/m^3 extends down to 20 km depth, slightly deepening in its western termination. The lower crust is rather thin all along the basin (5 km) with an average density of 2,950 kg/m^3. Therefore, the average density of the crust in the Pannonian Basin is between 2,790 and 2,800 kg/m^3. The model-predicted temperature at Moho levels beneath the Pannonian Basin varies from 500°C in the west to 450°C in the eastern part of the basin.

The Sava Suture Zone was modeled with an average density (2,850 kg/m^3) higher than in the surrounding crustal rocks (Figures 4 and 5).

5.2. LAB and Upper Mantle Characterization

In our best fi model, we distinguish three lithospheric mantle compositions (Figure 5). Beneath the Adriatic microplate (Adriatic mantle, Table 2 and Figure 5f) the lithospheric mantle composition corresponds to a slightly depleted mantle (Tc_2 of Griffin et al., 2009) with a mean Mg# of 89.5. In the Pannonian Basin (Tisza microplate) the composition of the mantle is the same as obtained by Alasonati Tašárová et al. (2016) and Downes et al. (1992) from the analysis of 20 xenoliths (Pannonian mantle, Table 2 and Figure 5f). Its mean Mg# of 90.4, which indicates the presence of a fertile mantle. The densities and seismic velocities resulting from these two lithospheric mantle compositions are very similar (with maximum differences of ∼10 kg/m^3 between densities and ∼0.01 km/s for V_p and V_s). However, we preferred maintaining the distinction between these different compositions to highlight the different tectonic history between the Adria and Tisza microplates. The third lithospheric mantle composition used is a residual DMM-3% composition (Mantle wedge, Table 2 and Figure 5f) beneath the External Apennines, Dinarides and Sava suture zone. This composition accounts for the presence of a mantle wedge and potential melting of the depleted asthenosphere (DMM) following rollback of the western (hereinafter Apenninic) and the eastern (hereinafter Dinaric) segments of the Adriatic slab. The sublithospheric mantle has been modeled using the DMM composition of Workman and Hart (2005) that is a reference model for an average, non-melted, depleted MORB mantle (more details in Kumar et al., 2020).

The LAB along the Adria microplate domain (Figure 5) is shallow (about 75 km depth) underneath the Tyrrhenian and Tuscany extended terrains and deeper (125–150 km depth) between the External Apennines and the Dinarides. In contrast to the Adriatic domain, the Tisza domain is characterized by a rather flat LAB (∼90 km), slightly deeper than the thermal LAB obtained by Artemieva (2019). Figure 5e compares the calculated LAB depth to the thermal LAB of Artemieva (2019) and to the S-RF and P-wave teleseismic LAB of Belinić et al. (2018) and Šumanovac and Dudjak (2016), respectively.

The resulting modeled densities and V_p and V_s seismic velocities for the assumed mantle compositions are shown in Figures 5f and 6. Under the same PT conditions, the density of the Adriatic mantle is slightly higher than that of the Pannonian mantle. Comparing the mantle density profiles of the Adriatic and Pannonian Basin we see that the density of the Adriatic mantle, for example, at 80 km depth, is higher, as much as 50 kg/m^3 than that of the Pannonian mantle (Figure 5). The lower values of mantle density are located at the base of the lithosphere in the Tuscany Magmatic Province (<3,280 kg/m^3) and in the Pannonian Basin (∼3,300 kg/m^3). Similarly, there is also a decrease of V_p and V_s from the Adriatic microplate to the Pannonian Basin (Figure 6c) as observed also by Belinić et al. (2021) at similar depths (Figure 3, panel b). The lowest seismic velocity is obtained in the lithospheric mantle of the Tuscany Magmatic Province with V_p and V_s values from 8.01 to 4.62 km/s below Moho depth to 7.8 and 4.32 km/s at LAB. The highest values of these velocities are found in the lithospheric mantle beneath the Adriatic Sea, with V_p between 8.15 and 8 km/s and V_s from 4.66 to 4.43 km/s. These differences in density and seismic velocity are mainly related to the LAB changes and, then, temperature distribution, more than to compositional changes.

The resulting density of the DMM-3% composition of the mantle wedge is much higher underneath the Dinarides/western Pannonian Basin area than underneath the Tyrrhenian-Tuscany region where the lithospheric thinning results in an increase of the thermal gradient and consequently a decrease in density and seismic velocities.

Furthermore, to better fit the geoid height and Bouguer anomaly (Figures 5b and 5c) and considering seismic tomographic results, we have modeled two sublithospheric thermo-compositional anomalies with an Adriatic mantle composition extending down to 400 km underneath the Apennines and to 250 km below the Dinarides. We keep the same chemical composition (Adriatic mantle) for both slabs considering that geophysical and geological

data point to the same Adriatic origin. The positive seismic velocity anomaly (2%–3%) beneath the northern Apennines (Figure 3 profile F-F' of panel A) (Giacomuzzi et al., 2011) and the increase of V_p (8.2–8.4 km/s) and V_s (4.6–4.8 km/s) velocities proposed by Belinić et al. (2021) underneath the Dinarides (Figure 3, panel 2) are both modeled as sublithospheric negative thermal mantle anomalies (−200°C) that extend down to 400 and 250 km, respectively. Our modeling shows that within the sublithospheric anomalies there is a 20 kg/m^3 increase in density (Figure 5f) and an increase of ∼1.5% for V_p and ∼2% for V_s. These thermo-compositional sublithospheric anomalies allow for a better adjustment not just with the seismic tomographic models but also with the geoid height and Bouguer anomaly (Figures 5b and 5c, blue and black lines).

6. Discussion

6.1. Crustal and Lithospheric Structure

The numerous geophysical surveys carried out in the study region allowed us to have a good constraint on the Moho depth along the northern Apennines and Dinarides (Figure 4 and references therein). Along the transect, we distinguish two main microplates, Adria and Tisza, separated by the Sava Suture to the east of the Dinarides. The geometry of the crustal layers produces the density variations required to fit the observables (Bouguer anomaly, geoid height, and elevation) and it is consistent with the geodynamic context.

The structure of the northern Apennines is complex and the Moho depth differs noticeably in different studies (e.g., Finetti et al., 2001; Liotta et al., 1998; Pauselli et al., 2006). Along the External Apennines, our results agree with those obtained by RFs studies (see references in Figure 4), where the Moho locally reaches maximum depths of ∼55 km, in an area where we modeled the top of the Apenninic slab (see next subsection). Beneath the Adriatic Sea, the Moho remains at a rather constant depth, consistent with the results of Molinari and Morelli (2011) and Grad et al. (2009). The Adria crust is deepening underneath the External Dinarides, where it is locally found at 45 km, in agreement with RF data (Stipčević et al., 2020; Šumanovac et al., 2016) and local earthquake tomography (Kapuralić et al., 2019).

According to Pamić et al. (2002) the Sava Suture Zone developed as a back-arc basin during the Cretaceous-Early Paleogene and was subsequently affected by Eocene collisional deformation and metamorphism accompanied by synkinematic granite plutonism, generation of an ophiolite mélange and finally thrusting onto the Dinarides. The high average density that we found for the Sava Suture zone agrees with this geologic history and it also explains the high-velocity body imaged by Kapuralić et al. (2019) at the transition between the Dinarides and the Pannonian Basin.

Figure 5e compares our calculated LAB depths to those reported in other studies. Although there is coincidence with previous models in the regional pattern of lithospheric thickness variations and in the depth of the LAB in the Tyrrhenian and Pannonian basins, there are discrepancies along the External Apennines and Dinarides and in the Adriatic Sea. The predicted LAB is similar to that of Artemieva (2019), except below the Apennines and the Adriatic Sea, likely due to the regional low resolution of Artemieva's model. In addition, our results agree with those of Šumanovac and Dudjak (2016) and Belinić et al. (2018) below the Dinarides, although significant differences are observed below the Pannonian Basin where we find a deeper LAB. The precise determination of the LAB depth depends on the measuring parameters. However, the different definitions should show a similar trend as all of them are imaging the rheologically strong outer layer of the Earth. Jiménez-Munt et al. (2019) found than seismic LAB roughly follows the 1,000°C ± 50°C isotherm. Along our profile, the trends obtained with different methods are similar, with the thermal LAB deeper than the seismic LAB. The seismic LAB from Šumanovac and Dudjak (2016) roughly follows the isotherm 1,000°C–900°C, whereas below the Dinarides the seimic LAB largely departs from this isotherm, probably related to the presence of the subducted cold slab, which is not in thermal equilibrium (Jiménez-Munt et al., 2019).

6.2. Mantle Composition and Anomalies

It is challenging to identify mantle chemical composition based on density and seismic velocities, because of the non-linear nature of the problem and the lack of uniqueness (Kumar et al., 2020). Hence, the composition of the mantle must be compatible with the geological and geodynamic history of the area. The composition of lithospheric mantle wedges is related to their backarc origin and to the degree of partial melting expected from

the nature and volume of magmatic events. The space opened between the trench and the upper plate during slab roll-back processes is replaced by a fertile sublithospheric mantle with DMM composition that will undergo partial melting by adiabatic decompression.

Our best fitting model requires two negative thermal anomalies in the upper mantle below the Apennines and Dinarides in agreement with the interpretation of seismic tomography images (e.g., Belinić et al., 2021; Benoit et al., 2011; El-Sharkawy et al., 2020; Giacomuzzi et al., 2011; Handy et al., 2021; Koulakov et al., 2015; Šumanovac et al., 2017). Beneath the Apennines, the best-fit model indicates the presence of a west-dipping attached cold lithospheric body down to 400 km, in continuation with the west dipping seismicity observed down to 70–80 km below the northern Apennines (De Luca et al., 2009). This deep cold body is characterized by seismic velocities anomalies between 1% and 2%, which coincide with those observed from the seismic tomography (e.g., Figure 3; Giacomuzzi et al., 2011; Kästle et al., 2020). The modeled low mantle velocities around 100 km depth in the Tuscany Magmatic Province (Figure 6) agree with the values (<−2%) predicted by the seismic tomography (e.g., Figure 3a).

Below the Dinarides, a much shorter 125 km-long and east-dipping mantle anomaly is required, resulting in a lithospheric slab down to 250 km. This result is in agreement with Šumanovac and Dudjak (2016), who image a pronounced fast velocity anomaly extending toward the NE direction to at least 250 km depth. Our favored model includes a mantle wedge below the Dinarides and southwest of the Pannonian basin, which is consistent with the S-wave low-velocity zone imaged from the inversion of Rayleigh-wave dispersion by Belinić et al. (2021) (Figure 3b).

6.3. Geodynamic Implications

The obtained transect across the northern Tyrrhenian Sea, northern Apennines, northern Dinarides and Pannonian Basin is compatible with previous studies, which indicate an initial configuration based on two main microplates: Adria and Tisza (e.g., Schmid et al., 2020). These microplates were separated by the N-S oriented Vardar Ocean, a Neo-Tethys oceanic branch, and interacted via subduction processes during Mesozoic and Cenozoic time in the framework of the convergence between Africa and Eurasia, which also led to the development of a SE-dipping Alpine-Tethys subduction related to the Alps.

The Adria microplate shows the most complex crustal structure since it encompasses both Apennines and Dinarides fold-thrust belts that show opposing vergence and are separated by the Adriatic Sea foreland. The Apennines orogenic system was built from Oligocene onwards by the deformation of the thinned western continental margin of Adria, after the consumption of the Ligurian-Alpine Tethys in a NW- and W-dipping subduction. This subduction was characterized by roll-back and, likely, later continental delamination, which led to the opening of the Liguro-Provencal and Tyrrhenian backarc basins (Figure 7). We interpret the sublithospheric anomaly observed in our model down to 400 km beneath the Apennines as the remnant slab after these processes. The eastern margin of Adria microplate was deformed over a much longer period spanning the Mesozoic and Cenozoic building of the Dinarides orogenic system (Schmid et al., 2008, 2020; Van Unen et al., 2019).

The Apennines thrust system geometry is still debated, since thin- and thick-skinned models have been proposed (e.g., Butler et al., 2004). Several studies propose that its most recent Neogene evolution is linked to east-directed rollback and subsequent delamination processes (e.g., Benoit et al., 2011; Chiarabba et al., 2014; D'Acquisto et al., 2020). The Internal Dinarides is composed by thrusted tectonic domains, including the Western Vardar Ophiolite Unit (e.g., Schmid et al., 2008), involving Mesozoic cover rocks belonging to the NE distal margin of Adria (Tari, 2002; Tomljenović et al., 2008). Jurassic obduction of Vadar oceanic crust is well preserved and well imaged in our crustal profile by a high-density body about 50 km wide and extending down to the base of the crust.

The northernmost Tyrrhenian Sea and western Tuscany, located onshore and corresponding to the Internal Apennines, are characterized by extensive magmatism (Tuscany Magmatic Province; e.g., Dini et al., 2002; Pandeli et al., 2013; Sani et al., 2016). The Tyrrhenian Sea in this region is characterized by a collection of scattered islands mainly formed by granitic intrusions, in which the largest Elba Island exposes the Monte Capanne and the apophysis of the Porto Azurro granite plutons with ages of 6.9 and 5.9 Ma (Figure 1a) (Pandeli et al., 2013). These granites were mostly derived from melting of the lower crust within an orogenic context (Peccerillo, 2005; Serri et al., 1993). Our crustal model is consistent with the presence of these granitic intrusions and volcanism,

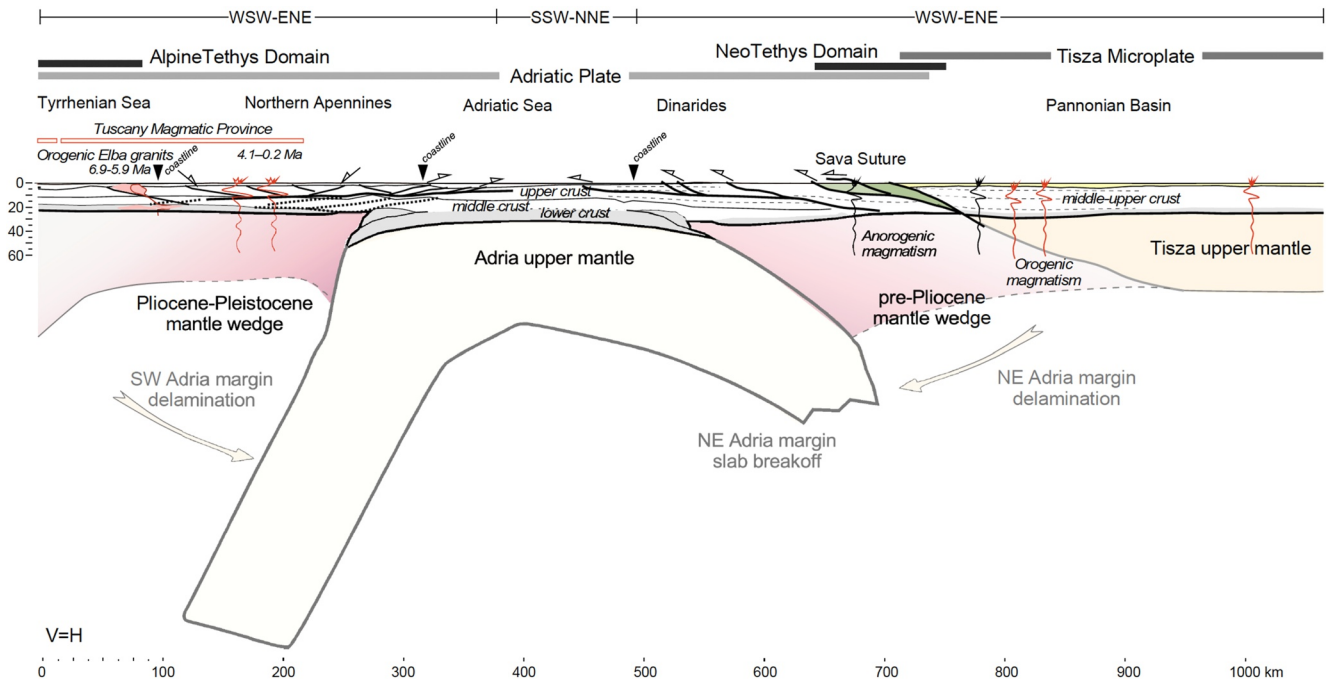

Figure 7. Modeled crust and upper mantle structure along the profile and our geodynamic interpretation.

which are the sources for high thermal conductivity and heat production in the area. The large Tuscany Magmatic Province onshore Italy formed from about 4 to 0.2 Ma extruding along the extensional system of normal faults thinning the Internal Apennines crust (Acocella & Rossetti, 2002). This is compatible with the results from our study, where the Tyrrhenian Sea and the western Apennines are characterized by high thermal gradient and thermal properties (conductivity and heat production) characteristic of magmatic rocks. Provided that continental collision occurred at about 25–30 Ma (e.g., Carminati et al., 2012), these magmatic rocks can be related to either roll-back of a continental slab or to delamination of Adria lithospheric mantle. Some authors proposed that delamination (in the sense of rollback of the lithospheric mantle slab) started at Corsica at about 15 Ma (e.g., Benoit et al., 2011), the resulting slab length should be consistent with the distance from the present-day west coast of Corsica to the crest of the northern Apennines. This distance agrees well with a 400 km deep slab, as modeled in the present study.

The crust is relatively thin below the Northern Tyrrhenian and it thickens toward the Internal-External Apennines boundary where west-dipping thrusts involve basement rocks. This simultaneous crustal thinning in the Tyrrhenian-Tuscan extended terrains and thickening in the External Apennines is consistent with eastward migrating continental subduction and with delamination, as widely acknowledged in the literature. The crust becomes thicker below the Adriatic foreland basin system along the Adriatic Sea, reaching maximum crustal thickness below the Internal Dinarides. This thick crust corresponds to the point of maximum bending of the eastern region of the Adriatic microplate.

The most interesting results, however, are the negative thermal anomalies required at the upper mantle below the Apennines and Dinarides. Beneath the Apennines, we find a west-dipping attached cold lithospheric body down to 400 km. We interpret this anomaly as the Apenninic slab, most likely generated by subduction rollback of oceanic and Adriatic continental lithosphere in a first stage, followed by continental lithospheric mantle delamination, in agreement with previous interpretations (e.g., Benoit et al., 2011; Chiarabba et al., 2014). Assuming only subduction rollback of such a long continental slab is less likely than rollback of the delaminated lithospheric mantle, due to the positive buoyancy of the continental crust.

Below the Dinarides, our model suggests a much shorter east-dipping mantle anomaly, resulting in a lithospheric slab down to 250 km. Šumanovac and Dudjak (2016) interpret this fast velocity anomaly as a downgoing lithosphere slab that has been detached from the crust, sinking steeply beneath the Dinarides. Moreover, our modeled mantle wedge below the Dinarides and southwest of the Pannonian basin is consistent with the low-velocity

zone imaged by Belinić et al. (2021). According to Belinić et al. (2021), the high velocity body indicates the possible delaminated lithospheric mantle slab, and the mentioned low-velocity zone the upwelling of hotter asthenospheric material, which agrees with our modeled cold sublithospheric anomaly and the mantle wedge. These two mantle anomalies are located far from the Ligurian Tethys and Vardar (Neo-Tethys) subduction zones. Therefore, these anomalies most likely represent sinking of continental lithosphere. Here we provide a unified view for the origin of these anomalies, as resulting from bidirectional post-collisional delamination of the Adriatic lithospheric mantle below the Apennines and the Dinarides orogens (Figure 7). Delamination related to the Apenninic slab resulted in a near vertical deeper slab and caused crustal and lithospheric thinning and partial melting in the Tyrrhenian-Tuscany region. The shallower anomaly beneath the Dinarides would be consistent with a shorter-lived delamination. On the basis of orogen-wide surface uplift of the Dinarides in Oligo-Miocene times and simultaneous emplacement of igneous rocks (33–22 Ma) in the Internal Dinarides, Balling et al. (2021) proposed post-collisional mantle delamination beginning at 28 Ma and terminated 22 Ma ago.

The thin lower crust below the Tuscany Magmatic Province and Dinarides and the current location of both slabs are compatible with their delamination once the continental collisions of Adria with Corsica Block and Tisza were accomplished with different ages and time lengths. The about 200°C colder bodies with respect to the surrounding rocks, their present size, position and coupling with shallower lithosphere have important consequences for both the evolution of the Apennines and Dinarides orogenic systems and the contribution to their recent dynamic topography.

The calculated isostatic elevation mostly matches the observed elevation except for the External Apennines, Dinarides and the Sava suture zone, where high-amplitude and medium to long-wavelength misfits are observed associated with the subducting slabs (Figure 5d). If we compute the effect of two end-member thermal isostatic models, with and without considering the effect of the sublithospheric anomalies, we observe that in the Apennines and Dinarides the slab deflects the elevation as much as 1,500 m (Figure 5d). This effect is to be expected since as mentioned the sublithospheric velocity anomalies (see Figure 3) are modeled as two thermal anomalies of −200°C (Figures 5 and 6) that result in a colder and higher density zone than the surrounding sublithospheric mantle. Moreover, the thick lithosphere below the Adriatic Sea and the two deepening slabs at both edges pull down the topography of the Adriatic microplate below sea level. For most of the profile, assuming regional isostasy with an elastic thickness (Te) between 10 and 20 km considerably reduces the mismatch between observed and calculated elevation (Figure 5d). The resulting Te agrees with the values obtained by Tesauro et al. (2009), based on thermal and rheological data, which are in the range of 10–20 km along the Tyrrhenian, Apennines and Pannonian Basin, and 20–25 km along the Adriatic Basin and Dinarides (Figure 3 of Tesauro et al., 2009).

7. Conclusions

We present a geophysical-petrological model of the crust and upper mantle structure along a transect extending from the northern Tyrrhenian Sea to the Pannonian Basin, crossing the northern Apennines and the northern Dinarides fold-thrust belts. The model offers an integrated view of the complex structure of Adria and Tisza microplates and of the west- and east-dipping slabs occurring along both sides of the Adriatic foreland, building the Apennines and Dinarides orogenic systems. From our results we can draw the following conclusions:

- Adria and Tisza microplates bounded by the Sava Suture Zone have a better fit with the model if they are distinguished by different densities. The best fitting average density for the Adria crust is 2,830 kg/m^3 whereas the Tisza crust shows a lower average density between 2,790 and 2,800 kg/m^3. This is partly because the lower crust of the Tisza plate is much thinner than that of Adria. The Tyrrhenian Sea and the Internal Apennines are characterized by the presence of elevated temperatures at shallow crustal levels, which is consistent with well-documented magmatic intrusions. We also observe that the crustal structure of the Adria microplate is more complex than that of the Tisza plate, particularly near the collisional zones showing that subduction/delamination in the area has mainly influenced the Adria domain. This is also observed at Moho levels, where major discrepancies between seismic data are found below the External Apennines and Dinarides. Our modeling permits us to solve these discrepancies and conclude that along the Internal Apennines the Moho lies at depths <25 km while along the External Apennines the Moho is found a depth of 55 km.
- The LAB shows significant lateral variations mainly related to the two crustal domains, recording their different tectonic evolution from the Mesozoic onwards. Beneath the Tyrrhenian Sea the LAB is flat and shallow at ∼75 km, slightly deepening toward the westernmost end of the profile. Below the Pannonian Basin the LAB

remains quite flat although ~20 km deeper than the seismic one. Along the External Apennines and Dinarides we observe that the LAB deepens to 150 km depth but shallowing toward the Adriatic foreland basin reaching 125 km depth.

- Two thermo-compositional sublithospheric anomalies with a T anomaly of −200°C relative to the surrounding mantle and with the same composition as the Adria lithospheric mantle are required to fit the geoid height and tomography studies. The presence of these thermal anomalies increases the density by 15–20 kg/m^3 allowing for a better fit of the geoid height and gravity anomaly and it is enough to reproduce the observed V_p and V_s anomalies. Below the Apennines, the west-dipping attached cold lithospheric slab reaches 400 km depth, which supports tomography models that favor the presence of a deep and cold anomaly as opposed to models that propose a shallower slab. Below the Dinarides, the east-dipping sublithospheric anomaly is shorter ending at 250 km depth, which agrees with seismic tomographic models.
- The lateral Adria LAB changes and the bidirectional sublithospheric anomalies below the Apennines and Dinarides are responsible for the resulting elevation, with low values in the Adriatic Sea due to its thick lithospheric mantle and the pulling down effect of the sublithospheric anomalies. Most of the elevation along the profile is under thermal isostasy. The observed elevation in the External Apennines, Dinarides and Sava Suture Zone can be explained assuming regional isostasy with an elastic thickness between 10 and 20 km.
- The model is compatible with two different lithospheric mantle compositions, a re-enriched basalt layer beneath the entire Adria microplate and a fertile mantle for the Tisza microplate lithospheric mantle. Moreover, the modeled lithospheric mantle composition below the Apennines and Dinarides is fertile compared to that of the rest of Adria and Tisza microplates. This is consistent with the presence of two sublithospheric mantle wedges, resulting from the bidirectional delamination of the Adria lithospheric mantle.

Data Availability Statement

Software and data used in this work are open access and they can be found in references cited in the main text and figure captions. Data sets for this article are available in Digital CSIC (http://hdl.handle.net/10261/280680, http://dx.doi.org/10.20350/digitalCSIC/14759).

Acknowledgments
We are grateful to Associate Editor Peter DeCelles and two anonymous reviewers for their constructive and detailed comments. We thank Emanuel David Kästle for making Figure 3c, Tena Belinic and co-authors for sharing their V_s model, and Eugenio Trumpy and Adele Manzella for providing us the Geothermal Database obtained within Geothopica Project. This work is funded by GeoCAM (PGC2018-095154-B-I00) from the Spanish Government, the Generalitat de Catalunya Grant (AGAUR 2017 SGR 847) and ALORBE (PIE-CSIC-202030E10). WZ is supported by the China Scholarship Council (CSC-201904910470) and EBG by the Spanish Government Grant PRE2019-090524. This work has been done using the facilities of the Laboratory of Geodynamic Modeling from Geo3BCN-CSIC. Figures were made with the Generic Mapping Tools (www.soest.hawaii.edu/gmt; Wessel & Smith, 1998).

References

Acocella, V., & Rossetti, F. (2002). The role of extensional tectonics at different crustal levels on granite ascent and emplacement: An example from Tuscany (Italy). *Tectonophysics*, *354*(1), 71–83. https://doi.org/10.1016/S0040-1951(02)00290-1

Afonso, J. C., Fernàndez, M., Ranalli, G., Griffin, W. L., & Connolly, J. A. D. (2008). Integrated geophysical-petrological modeling of the lithosphere and sublithospheric upper mantle: Methodology and applications. *Geochemistry, Geophysics, Geosystems*, *9*(5), Q05008. https://doi.org/10.1029/2007GC001834

Alasonati Tašárová, Z., Fullea, J., Bielik, M., & Środa, P. (2016). Lithospheric structure of Central Europe: Puzzle pieces from Pannonian Basin to trans-European Suture Zone resolved by geophysical-petrological modeling: Geophysical-petrological modeling. *Tectonics*, *35*(3), 722–753. https://doi.org/10.1002/2015TC003935

Amaru, M. L. (2007). *Global travel time tomography with 3-D reference models*. Utrecht University. Retrieved from http://dspace.library.uu.nl/handle/1874/19338

Artemieva, I. M. (2019). Lithosphere thermal thickness and geothermal heat flux in Greenland from a new thermal isostasy method. *Earth-Science Reviews*, *188*, 469–481. https://doi.org/10.1016/j.earscirev.2018.10.015

Artemieva, I. M., & Thybo, H. (2013). EUNAseis: A seismic model for Moho and crustal structure in Europe, Greenland, and the North Atlantic region. *Tectonophysics*, *609*, 97–153. https://doi.org/10.1016/j.tecto.2013.08.004

Bada, G., Horváth, F., Dövényi, P., Szafián, P., Windhoffer, G., & Cloetingh, S. (2007). Present-day stress field and tectonic inversion in the Pannonian basin. *Global and Planetary Change*, *58*(1), 165–180. https://doi.org/10.1016/j.gloplacha.2007.01.007

Balling, P., Tomljenović, B., Schmid, S. M., & Ustaszewski, K. (2021). Contrasting along-strike deformation styles in the central external Dinarides assessed by balanced cross-sections: Implications for the tectonic evolution of its Paleogene flexural foreland basin system. *Global and Planetary Change*, *205*, 103587. https://doi.org/10.1016/j.gloplacha.2021.103587

Bally, A. W. (1987). Balanced sections and seismic reflection profiles across the Central Apennines, Italy. *Memoirs Geological Society Italy*, *29*(8), 11–12.

Barchi, M., Minelli, G., Magnani, B., & Mazzotti, A. (2003). Line CROP 03: Northern Apennines. In *Memorie Descrittive della Carta geologica d'Italia LXII* (Vol. *62*, pp. 127–136).

Barchi, M., Minelli, G., & Pialli, G. (1998). The Crop 03 profile: A synthesis of results on deep structures of the Northern Apennines. *Memorie della Societa Geologica Italiana*, *52*, 383–400.

Barchi, M., Pauselli, C., Chiarabba, C., Di Stefano, R., Federico, C., & Minelli, G. (2006). Crustal structure, tectonic evolution and seismogenesis in the Northern Apennines (Italy). *Bollettino di Geofisica Teorica ed Applicata*, *47*, 249–270.

Barchi, M. R., Carboni, F., Michele, M., Ercoli, M., Giorgetti, C., Porreca, M., et al. (2021). The influence of subsurface geology on the distribution of earthquakes during the 2016–2017 Central Italy seismic sequence. *Tectonophysics*, *807*, 228797. https://doi.org/10.1016/j.tecto.2021.228797

Basili, R., & Barba, S. (2007). Migration and shortening rates in the northern Apennines, Italy: Implications for seismic hazard. *Terra Nova*, *19*(6), 462–468. https://doi.org/10.1111/j.1365-3121.2007.00772.x

Belinić, T., Kolínský, P., & Stipčević, J. (2021). Shear-wave velocity structure beneath the Dinarides from the inversion of Rayleigh-wave dispersion. *Earth and Planetary Science Letters*, *555*, 116686. https://doi.org/10.1016/j.epsl.2020.116686

Belinić, T., Stipčević, J., & Živčić, M. (2018). Lithospheric thickness under the Dinarides. *Earth and Planetary Science Letters*, *484*, 229–240. https://doi.org/10.1016/j.epsl.2017.12.030

Beller, S., Monteiller, V., Operto, S., Nolet, G., Paul, A., & Zhao, L. (2018). Lithospheric architecture of the South-Western Alps revealed by multiparameter teleseismic full-waveform inversion. *Geophysical Journal International*, *212*(2), 1369–1388. https://doi.org/10.1093/gji/ggx216

Benoit, M. H., Torpey, M., Liszewski, K., Levin, V., & Park, J. (2011). P and S wave upper mantle seismic velocity structure beneath the northern Apennines: New evidence for the end of subduction. *Geochemistry, Geophysics, Geosystems*, *12*(6), Q06004. https://doi.org/10.1029/2010GC003428

Bianco, C., Brogi, A., Caggianelli, A., Giorgetti, G., Liotta, D., & Meccheri, M. (2015). HP-LT metamorphism in Elba island: Implications for the geodynamic evolution of the inner Northern Apennines (Italy). *Journal of Geodynamics*, *91*, 13–25. https://doi.org/10.1016/j.jog.2015.08.001

Blom, N., Gokhberg, A., & Fichtner, A. (2020). Seismic waveform tomography of the central and eastern Mediterranean upper mantle. *Solid Earth*, *11*(2), 669–690. https://doi.org/10.5194/se-11-669-2020

Boccaletti, M., Ciaranfi, N., Cosentino, D., Deiana, G., Gelati, R., Lentini, F., et al. (1990). Palinspastic restoration and paleogeographic reconstruction of the peri-Tyrrhenian area during the Neogene. *Palaeogeography, Palaeoclimatology, Palaeoecology*, *77*(1), 41-IN13–IN13. https://doi.org/10.1016/0031-0182(90)90097-Q

Bondár, I., Mónus, P., Czanik, C., Kiszely, M., Gráczer, Z., & Wéber, Z., & the AlpArrayWorking Group. (2018). Relocation of seismicity in the Pannonian basin using a global 3D velocity model. *Seismological Research Letters*, *89*(6), 2284–2293. https://doi.org/10.1785/0220180143

Bonini, M., & Sani, F. (2002). Extension and compression in the Northern Apennines (Italy) hinterland: Evidence from the late Miocene-Pliocene Siena-Radicofani Basin and relations with basement structures. *Tectonics*, *21*(3), 1-1–1-32. https://doi.org/10.1029/2001TC900024

Brocher, T. M. (2005). Empirical relations between elastic wavespeeds and density in the Earth's crust. *Bulletin of the Seismological Society of America*, *95*(6), 2081–2092. https://doi.org/10.1785/0120050077

Butler, R. W. H., Mazzoli, S., Corrado, S., De Donatis, M., Di Bucci, D., Gambini, R., et al. (2004). Applying thick-skinned tectonic models to the Apennine thrust belt of Italy—Limitations and implications.

Carballo, A., Fernandez, M., Torne, M., Jiménez-Munt, I., & Villaseñor, A. (2015). Thermal and petrophysical characterization of the lithospheric mantle along the northeastern Iberia geo-transect. *Gondwana Research*, *27*(4), 1430–1445. https://doi.org/10.1016/j.gr.2013.12.012

Carminati, E., & Doglioni, C. (2012). Alps vs. Apennines: The paradigm of a tectonically asymmetric Earth. *Earth-Science Reviews*, *112*(1), 67–96. https://doi.org/10.1016/j.earscirev.2012.02.004

Carminati, E., Lustrino, M., & Doglioni, C. (2012). Geodynamic evolution of the central and western Mediterranean: Tectonics vs. igneous petrology constraints. *Tectonophysics*, *579*, 173–192. https://doi.org/10.1016/j.tecto.2012.01.026

Carminati, E., Petricca, P., & Doglioni, C. (2020). Mediterranean tectonics. In D. Alderton & S. A. Elias (Eds.), *Encyclopedia of geology* (2nd ed., pp. 408–419). Academic Press. https://doi.org/10.1016/B978-0-08-102908-4.00010-2

Cassinis, R., Scarascia, S., Lozej, A., & Finetti, I. R. (2005). Review of seismic wide-angle reflection–refraction (WARR) results in the Italian region (1956–1987). In *CROP project: Deep seismic exploration of the central Mediterranean and Italy* (pp. 31–55). Elsevier Amsterdam.

Cavinato, G. P., & DeCelles, P. (1999). Extensional basins in the tectonically bimodal central Apennines fold-thrust belt, Italy: Response to corner flow above a subducting slab in retrograde motion. *Geology*, *27*(10), 955–958. https://doi.org/10.1130/0091-7613(1999)027<0955:ebittb>2.3.co;2

Channell, J. E. T., Tüysüz, O., Bektas, O., & Sengör, A. M. C. (1996). Jurassic-Cretaceous paleomagnetism and paleogeography of the Pontides (Turkey). *Tectonics*, *15*(1), 201–212. https://doi.org/10.1029/95TC02290

Chiarabba, C., Bianchi, I., De Gori, P., & Agostinetti, N. P. (2020). Mantle upwelling beneath the Apennines identified by receiver function imaging. *Scientific Reports*, *10*(1), 19760. https://doi.org/10.1038/s41598-020-76515-2

Chiarabba, C., Giacomuzzi, G., Bianchi, I., Agostinetti, N. P., & Park, J. (2014). From underplating to delamination-retreat in the northern Apennines. *Earth and Planetary Science Letters*, *403*, 108–116. https://doi.org/10.1016/j.epsl.2014.06.041

Chiarabba, C., Jovane, L., & DiStefano, R. (2005). A new view of Italian seismicity using 20 years of instrumental recordings. *Tectonophysics*, *395*(3), 251–268. https://doi.org/10.1016/j.tecto.2004.09.013

Chiarabba, C., Pino, N. A., Ventura, G., & Vilardo, G. (2004). Structural features of the shallow plumbing system of Vulcano Island Italy. *Bulletin of Volcanology*, *66*(6), 477–484. https://doi.org/10.1007/s00445-003-0331-9

Chiari, M., Djerić, N., Garfagnoli, F., Hrvatović, H., Krstić, M., Levi, N., et al. (2011). The geology of the Zlatibor-Maljen area (western Serbia): A geotraverse across the ophiolites of the Dinaric-Hellenic collisional belt. *Ofioliti*, *36*(2), 139–166. https://doi.org/10.4454/OFIOLITI.V36.I2.3

Collettini, C., & Barchi, M. R. (2002). A low-angle normal fault in the Umbria region (Central Italy): A mechanical model for the related microseismicity. *Tectonophysics*, *359*(1–2), 97–115. https://doi.org/10.1016/s0040-1951(02)00441-9

Connolly, J. A. D. (2005). Computation of phase equilibria by linear programming: A tool for geodynamic modeling and its application to subduction zone decarbonation. *Earth and Planetary Science Letters*, *236*(1), 524–541. https://doi.org/10.1016/j.epsl.2005.04.033

Connolly, J. A. D. (2009). The geodynamic equation of state: What and how. *Geochemistry, Geophysics, Geosystems*, *10*(10), Q10014. https://doi.org/10.1029/2009GC002540

Conti, P., Cornamusini, G., & Carmignani, L. (2020). An outline of the geology of the northern Apennines (Italy), with geological map at 1: 250,000 scale. *Italian Journal of Geosciences*, *139*(2), 149–194. https://doi.org/10.3301/ijg.2019.25

Cosentino, D., Cipollari, P., Marsili, P., & Scrocca, D. (2010). Geology of the central Apennines: A regional review. *Journal of the Virtual Explorer*, *36*, 1–37. https://doi.org/10.3809/jvirtex.2010.00223

Coward, M. P., De Donatis, M., Mazzoli, S., Paltrinieri, W., & Wezel, F. C. (1999). Frontal part of the northern Apennines fold and thrust belt in the Romagna-Marche area (Italy): Shallow and deep structural styles. *Tectonics*, *18*(3), 559–574. https://doi.org/10.1029/1999TC900003

Csontos, L., & Nagymarosy, A. (1998). The Mid-Hungarian line: A zone of repeated tectonic inversions. *Tectonophysics*, *297*(1), 51–71. https://doi.org/10.1016/S0040-1951(98)00163-2

Cuffaro, M., Riguzzi, F., Scrocca, D., Antonioli, F., Carminati, E., Livani, M., & Doglioni, C. (2010). On the geodynamics of the northern Adriatic plate. *Rendiconti Lincei*, *21*(1), 253–279. https://doi.org/10.1007/s12210-010-0098-9

Curzi, M., Aldega, L., Bernasconi, S. M., Berra, F., Billi, A., Boschi, C., et al. (2020). Architecture and evolution of an extensionally-inverted thrust (Mt. Tancia Thrust, Central Apennines): Geological, structural, geochemical, and K–Ar geochronological constraints. *Journal of Structural Geology*, *136*, 104059. https://doi.org/10.1016/j.jsg.2020.104059

D'Acquisto, M., Dal Zilio, L., Molinari, I., Kissling, E., Gerya, T., & van Dinther, Y. (2020). Tectonics and seismicity in the northern Apennines driven by slab retreat and lithospheric delamination. *Tectonophysics*, *789*, 228481. https://doi.org/10.1016/j.tecto.2020.228481

De Luca, G., Cattaneo, M., Monachesi, G., & Amato, A. (2009). Seismicity in central and northern Apennines integrating the Italian national and regional networks. *Tectonophysics*, *476*(1), 121–135. https://doi.org/10.1016/j.tecto.2008.11.032

Dewey, J. F., Helman, M. L., Knott, S. D., Turco, E., & Hutton, D. H. W. (1989). Kinematics of the western Mediterranean. *Geological Society, London, Special Publications*, *45*(1), 265–283. https://doi.org/10.1144/GSL.SP.1989.045.01.15

Diaferia, G., Cammarano, F., Piana Agostinetti, N., Gao, C., Lekic, V., Molinari, I., & Boschi, L. (2019). Inferring Crustal temperatures beneath Italy from joint inversion of receiver functions and surface waves. *Journal of Geophysical Research: Solid Earth*, *124*(8), 8771–8785. https://doi.org/10.1029/2019JB018340

Dini, A., Gianelli, G., Puxeddu, M., & Ruggieri, G. (2005). Origin and evolution of Pliocene–Pleistocene granites from the Larderello geothermal field (Tuscan Magmatic Province, Italy). *Lithos*, *81*(1), 1–31. https://doi.org/10.1016/j.lithos.2004.09.002

Dini, A., Innocenti, F., Rocchi, S., Tonarini, S., & Westerman, D. S. (2002). The magmatic evolution of the late Miocene laccolith–pluton–dyke granitic complex of Elba Island, Italy. *Geological Magazine*, *139*(3), 257–279. https://doi.org/10.1017/S0016756802006556

Doglioni, C. (1991). A proposal for the kinematic modelling of W-dipping subductions—Possible applications to the Tyrrhenian-Apennines system. *Terra Nova*, *3*(4), 423–434. https://doi.org/10.1111/j.1365-3121.1991.tb00172.x

Doglioni, C., Gueguen, E., Sàbat, F., & Fernandez, M. (1997). The western Mediterranean extensional basins and the Alpine orogen. *Terra Nova*, *9*(3), 109–112. https://doi.org/10.1046/j.1365-3121.1997.d01-18.x

Doglioni, C., Harabaglia, P., Martinelli, G., Mongelli, F., & Zito, G. (1996). A geodynamic model of the Southern Apennines accretionary prism. *Terra Nova*, *8*(6), 540–547. https://doi.org/10.1111/j.1365-3121.1996.tb00783.x

Downes, H., Embey-Isztin, A., & Thirlwall, M. F. (1992). Petrology and geochemistry of spinel peridotite xenoliths from the western Pannonian Basin (Hungary): Evidence for an association between enrichment and texture in the upper mantle. *Contributions to Mineralogy and Petrology*, *109*(3), 340–354. https://doi.org/10.1007/BF00283323

El-Sharkawy, A., Meier, T., Lebedev, S., Behrmann, J. H., Hamada, M., Cristiano, L., et al. (2020). The slab puzzle of the Alpine-Mediterranean region: Insights from a new, high-resolution, shear wave velocity model of the upper mantle. *Geochemistry, Geophysics, Geosystems*, *21*(8), e2020GC008993. https://doi.org/10.1029/2020GC008993

Faccenna, C., Becker, T. W., Auer, L., Billi, A., Boschi, L., Brun, J. P., et al. (2014). Mantle dynamics in the Mediterranean. *Reviews of Geophysics*, *52*(3), 283–332. https://doi.org/10.1002/2013RG000444

Faccenna, C., Becker, T. W., Lucente, F. P., Jolivet, L., & Rossetti, F. (2001). History of subduction and back arc extension in the Central Mediterranean. *Geophysical Journal International*, *145*(3), 809–820. https://doi.org/10.1046/j.0956-540x.2001.01435.x

Fantoni, R., & Franciosi, R. (2010). Tectono-sedimentary setting of the Po plain and Adriatic foreland. *Rendiconti Lincei*, *21*(1), 197–209. https://doi.org/10.1007/s12210-010-0102-4

Fernàndez, M., Afonso, J. C., & Ranalli, G. (2010). The deep lithospheric structure of the Namibian volcanic margin. *Tectonophysics*, *481*(1–4), 68–81. https://doi.org/10.1016/j.tecto.2009.02.036

Finetti, I. R., Boccaletti, M., Bonini, M., Del Ben, A., Geletti, R., Pipan, M., & Sani, F. (2001). Crustal section based on CROP seismic data across the North Tyrrhenian–Northern Apennines–Adriatic Sea. *Tectonophysics*, *343*(3), 135–163. https://doi.org/10.1016/S0040-1951(01)00141-X

Fuchs, S., & Norden, B. (2021). The global heat flow database: Release 2021. https://doi.org/10.5880/fidgeo.2021.014

Fullea, J., Fernàndez, M., & Zeyen, H. (2008). FA2BOUG—A FORTRAN 90 code to compute Bouguer gravity anomalies from gridded free-air anomalies: Application to the Atlantic-Mediterranean transition zone. *Computers & Geosciences*, *34*(12), 1665–1681. https://doi.org/10.1016/j.cageo.2008.02.018

Gallhofer, D., von Quadt, A., Schmid, S. M., Guillong, M., Peytcheva, I., & Seghedi, I. (2017). Magmatic and tectonic history of Jurassic ophiolites and associated granitoids from the South Apuseni Mountains (Romania). *Swiss Journal of Geosciences*, *110*(2), 699–719. https://doi.org/10.1007/s00015-016-0231-6

Geissler, W. H., Sodoudi, F., & Kind, R. (2010). Thickness of the central and eastern European lithosphere as seen by S receiver functions. *Geophysical Journal International*, *181*(2), 604–634. https://doi.org/10.1111/j.1365-246X.2010.04548.x

Ghielmi, M., Minervini, M., Nini, C., Rogledi, S., Rossi, M., & Vignolo, A. (2010). Sedimentary and tectonic evolution in the eastern Po-plain and northern Adriatic Sea area from Messinian to Middle Pleistocene (Italy). *Rendiconti Lincei*, *21*(1), 131–166. https://doi.org/10.1007/s12210-010-0101-5

Giacomuzzi, G., Chiarabba, C., & De Gori, P. (2011). Linking the Alps and Apennines subduction systems: New constraints revealed by high-resolution teleseismic tomography. *Earth and Planetary Science Letters*, *301*(3), 531–543. https://doi.org/10.1016/j.epsl.2010.11.033

Gilardoni, M., Reguzzoni, M., & Sampietro, D. (2016). GECO: A global gravity model by locally combining GOCE data and EGM2008. *Studia Geophysica et Geodaetica*, *60*(2), 228–247. https://doi.org/10.1007/s11200-015-1114-4

Grad, M., & Tiira, T., & ESC Working Group. (2009). The Moho depth map of the European Plate. *Geophysical Journal International*, *176*(1), 279–292. https://doi.org/10.1111/j.1365-246X.2008.03919.x

Griffin, W. L., O'Reilly, S. Y., Afonso, J. C., & Begg, G. C. (2009). The composition and evolution of lithospheric mantle: A re-evaluation and its tectonic implications. *Journal of Petrology*, *50*(7), 1185–1204. https://doi.org/10.1093/petrology/egn033

Handy, M. R., Schmid, S. M., Bousquet, R., Kissling, E., & Bernoulli, D. (2010). Reconciling plate-tectonic reconstructions of Alpine Tethys with the geological–geophysical record of spreading and subduction in the Alps. *Earth-Science Reviews*, *102*(3), 121–158. https://doi.org/10.1016/j.earscirev.2010.06.002

Handy, M. R., Schmid, S. M., Paffrath, M., & Friederich, W., & the AlpArray Working Group. (2021). Orogenic lithosphere and slabs in the greater Alpine area—Interpretations based on teleseismic P-wave tomography. *Solid Earth*, *12*(11), 2633–2669. https://doi.org/10.5194/se-12-2633-2021

Handy, M. R., Ustaszewski, K., & Kissling, E. (2015). Reconstructing the Alps–Carpathians–Dinarides as a key to understanding switches in subduction polarity, slab gaps and surface motion. *International Journal of Earth Sciences*, *104*(1), 1–26. https://doi.org/10.1007/s00531-014-1060-3

Hetényi, G., Ren, Y., Dando, B., Stuart, G. W., Hegedűs, E., Kovács, A. C., & Houseman, G. A. (2015). Crustal structure of the Pannonian Basin: The AlCaPa and Tisza terrains and the Mid-Hungarian zone. *Tectonophysics*, *646*, 106–116. https://doi.org/10.1016/j.tecto.2015.02.004

Horváth, F. (1995). Phases of compression during the evolution of the Pannonian Basin and its bearing on hydrocarbon exploration. *Marine and Petroleum Geology*, *12*(8), 837–844. https://doi.org/10.1016/0264-8172(95)98851-U

Horváth, F., Bada, G., Szafián, P., Tari, G., Ádám, A., & Cloetingh, S. (2006). Formation and deformation of the Pannonian Basin: Constraints from observational data. *Geological Society, London, Memoirs*, *32*(1), 191–206. https://doi.org/10.1144/GSL.MEM.2006.032.01.11

Hua, Y., Zhao, D., & Xu, Y. (2017). P wave anisotropic tomography of the Alps. *Journal of Geophysical Research: Solid Earth*, *122*(6), 4509–4528. https://doi.org/10.1002/2016JB013831

Jiménez-Munt, I., Torne, M., Fernàndez, M., Vergés, J., Kumar, A., Carballo, A., & García-Castellanos, D. (2019). Deep seated density anomalies across the Iberia-Africa plate boundary and its topographic response. *Journal of Geophysical Research: Solid Earth*, *124*(12), 13310–13332. https://doi.org/10.1029/2019JB018445

Jolivet, L., Faccenna, C., Goffé, B., Mattei, M., Rossetti, F., Brunet, C., et al. (1998). Midcrustal shear zones in postorogenic extension: Example from the northern Tyrrhenian Sea. *Journal of Geophysical Research*, *103*(B6), 12123–12160. https://doi.org/10.1029/97JB03616

Kapuralić, J., Šumanovac, F., & Markušić, S. (2019). Crustal structure of the northern Dinarides and southwestern part of the Pannonian basin inferred from local earthquake tomography. *Swiss Journal of Geosciences*, *112*(1), 181–198. https://doi.org/10.1007/s00015-018-0335-2

Kästle, E. D., El-Sharkawy, A., Boschi, L., Meier, T., Rosenberg, C., Bellahsen, N., et al. (2018). Surface wave tomography of the Alps using ambient-noise and earthquake phase velocity measurements. *Journal of Geophysical Research: Solid Earth*, *123*(2), 1770–1792. https://doi.org/10.1002/2017JB014698

Kästle, E. D., Molinari, I., Boschi, L., & Kissling, E., & the AlpArray Working Group. (2022). Azimuthal anisotropy from eikonal tomography: Example from ambient-noise measurements in the AlpArray network. *Geophysical Journal International*, *229*(1), 151–170. https://doi.org/10.1093/gji/ggab453

Kästle, E. D., Rosenberg, C., Boschi, L., Bellahsen, N., Meier, T., & El-Sharkawy, A. (2020). Slab break-offs in the Alpine subduction zone. *International Journal of Earth Sciences*, *109*(2), 587–603. https://doi.org/10.1007/s00531-020-01821-z

Keller, J. V. A., & Coward, M. P. (1996). The structure and evolution of the northern Tyrrhenian Sea. *Geological Magazine*, *133*(1), 1–16. https://doi.org/10.1017/S0016756800007214

Keller, J. V. A., Minelli, G., & Pialli, G. (1994). Anatomy of late orogenic extension: The Northern Apennines case. *Tectonophysics*, *238*(1), 275–294. https://doi.org/10.1016/0040-1951(94)90060-4

Korbar, T. (2009). Orogenic evolution of the External Dinarides in the NE Adriatic region: A model constrained by tectonostratigraphy of Upper Cretaceous to Paleogene carbonates. *Earth-Science Reviews*, *96*(4), 296–312. https://doi.org/10.1016/j.earscirev.2009.07.004

Koroknai, B., Wórum, G., Tóth, T., Koroknai, Z., Fekete-Németh, V., & Kovács, G. (2020). Geological deformations in the Pannonian basin during the neotectonic phase: New insights from the latest regional mapping in Hungary. *Earth-Science Reviews*, *211*, 103411. https://doi.org/10.1016/j.earscirev.2020.103411

Koulakov, I., Jakovlev, A., Zabelina, I., Roure, F., Cloetingh, S., El Khrepy, S., & Al-Arifi, N. (2015). Subduction or delamination beneath the Apennines? Evidence from regional tomography. *Solid Earth*, *6*(2), 669–679. https://doi.org/10.5194/se-6-669-2015

Koulakov, I., Kaban, M. K., Tesauro, M., & Cloetingh, S. (2009). P- and S-velocity anomalies in the upper mantle beneath Europe from tomographic inversion of ISC data. *Geophysical Journal International*, *179*(1), 345–366. https://doi.org/10.1111/j.1365-246X.2009.04279.x

Kovács, I., Csontos, L., Szabó, C. S., Bali, E., Falus, G., Benedek, K., & Zajacz, Z. (2007). Paleogene–early Miocene igneous rocks and geodynamics of the Alpine-Carpathian-Pannonian-Dinaric region: An integrated approach. In L. Beccaluva, G. Bianchini, & M. Wilson (Eds.), *Cenozoic volcanism in the Mediterranean area*. Geological Society of America. https://doi.org/10.1130/2007.2418(05)

Kuk, V., Prelogović, E., & Dragičević, I. (2000). Seismotectonically active zones in the Dinarides. *Geologia Croatica*, *53*(2), 295–303.

Kumar, A., Fernàndez, M., Jiménez-Munt, I., Torne, M., Vergés, J., & Afonso, J. C. (2020). LitMod2D_2.0: An improved integrated geophysical-petrological modeling tool for the physical interpretation of upper mantle anomalies. *Geochemistry, Geophysics, Geosystems*, *21*(3), e2019GC008777. https://doi.org/10.1029/2019GC008777

Kumar, A., Fernàndez, M., Vergés, J., Torne, M., & Jiménez-Munt, I. (2021). Opposite symmetry in the lithospheric structure of the Alboran and Algerian basins and their margins (Western Mediterranean): Geodynamic implications. *Journal of Geophysical Research: Solid Earth*, *126*(7), e2020JB021388. https://doi.org/10.1029/2020JB021388

Lacombe, O., & Jolivet, L. (2005). Structural and kinematic relationships between Corsica and the Pyrenees-Provence domain at the time of the Pyrenean orogeny. *Tectonics*, *24*(1). https://doi.org/10.1029/2004TC001673

Laske, G., Masters, G., Ma, Z., & Pasyanos, M. (2013). Update on CRUST1.0—A 1-degree global model of Earth's Crust. In *Geophysical research abstracts EGU2013-2658* (Vol. *15*).

Le Breton, E., Handy, M. R., Molli, G., & Ustaszewski, K. (2017). Post-20 Ma motion of the Adriatic Plate: New Constraints from surrounding orogens and implications for crust-mantle Decoupling. *Tectonics*, *36*(12), 3135–3154. https://doi.org/10.1002/2016TC004443

Liotta, D., Cernobori, L., & Nicolich, R. (1998). Restricted rifting and its consistence with compressional structures: Results from CROP 3 traverse (Northern Apenninies, Italy). *Terra Nova*, *10*(1), 16–20. https://doi.org/10.1046/j.1365-3121.1998.00157.x

Lippitsch, R., Kissling, E., & Ansorge, J. (2003). Upper mantle structure beneath the Alpine orogen from high-resolution teleseismic tomography. *Journal of Geophysical Research*, *108*(B8), 2376. https://doi.org/10.1029/2002JB002016

Lucente, F. P., Chiarabba, C., Cimini, G. B., & Giardini, D. (1999). Tomographic constraints on the geodynamic evolution of the Italian region. *Journal of Geophysical Research*, *104*(B9), 20307–20327. https://doi.org/10.1029/1999JB900147

Lustrino, M., Chiarabba, C., & Carminati, E. (2022). *Igneous activity in central-southern Italy: Is the subduction paradigm still valid? In the footsteps of Warren B. Hamilton: New ideas in earth science*. Geological Society of America. https://doi.org/10.1130/2021.2553(28)

Maesano, F. E., Toscani, G., Burrato, P., Mirabella, F., D'Ambrogi, C., & Basili, R. (2013). Deriving thrust fault slip rates from geological modeling: Examples from the Marche coastal and offshore contraction belt, northern Apennines, Italy. *Marine and Petroleum Geology*, *42*, 122–134. https://doi.org/10.1016/j.marpetgeo.2012.10.008

Maffione, M., & van Hinsbergen, D. J. J. (2018). Reconstructing plate boundaries in the Jurassic neo-Tethys from the east and west Vardar ophiolites (Greece and Serbia). *Tectonics*, *37*(3), 858–887. https://doi.org/10.1002/2017TC004790

Malinverno, A., & Ryan, W. B. F. (1986). Extension in the Tyrrhenian Sea and shortening in the Apennines as result of arc migration driven by sinking of the lithosphere. *Tectonics*, *5*(2), 227–245. https://doi.org/10.1029/TC005i002p00227

Massoli, D., Koyi, H. A., & Barchi, M. R. (2006). Structural evolution of a fold and thrust belt generated by multiple décollements: Analogue models and natural examples from the Northern Apennines (Italy). *Journal of Structural Geology*, *28*(2), 185–199. https://doi.org/10.1016/j.jsg.2005.11.002

Matenco, L., & Radivojević, D. (2012). On the formation and evolution of the Pannonian Basin: Constraints derived from the structure of the junction area between the Carpathians and Dinarides. *Tectonics*, *31*(6), 6007. https://doi.org/10.1029/2012TC003206

Mazzoli, S., Pierantoni, P. P., Borraccini, F., Paltrinieri, W., & Deiana, G. (2005). Geometry, segmentation pattern and displacement variations along a major Apennine thrust zone, central Italy. *Journal of Structural Geology*, *27*(11), 1940–1953. https://doi.org/10.1016/j.jsg.2005.06.002

Mele, G., & Sandvol, E. (2003). Deep crustal roots beneath the northern Apennines inferred from teleseismic receiver functions. *Earth and Planetary Science Letters*, *211*(1), 69–78. https://doi.org/10.1016/S0012-821X(03)00185-7

Miller, M. S., & Piana Agostinetti, N. (2012). Insights into the evolution of the Italian lithospheric structure from S receiver function analysis. *Earth and Planetary Science Letters*, *345*(348), 49–59. https://doi.org/10.1016/j.epsl.2012.06.028

Moeller, S., Grevemeyer, I., Ranero, C. R., Berndt, C., Klaeschen, D., Sallares, V., et al. (2013). Early-stage rifting of the northern Tyrrhenian Sea Basin: Results from a combined wide-angle and multichannel seismic study. *Geochemistry, Geophysics, Geosystems*, *14*(8), 3032–3052. https://doi.org/10.1002/ggge.20180

Moeller, S., Grevemeyer, I., Ranero, C. R., Berndt, C., Klaeschen, D., Sallares, V., et al. (2014). Crustal thinning in the northern Tyrrhenian Rift: Insights from multichannel and wide-angle seismic data across the basin. *Journal of Geophysical Research: Solid Earth*, *119*(3), 1655–1677. https://doi.org/10.1002/2013JB010431

Molinari, I., & Morelli, A. (2011). EPcrust: A reference crustal model for the European plate. *Geophysical Journal International*, *185*(1), 352–364. https://doi.org/10.1111/j.1365-246X.2011.04940.x

Molinari, I., Verbeke, J., Boschi, L., Kissling, E., & Morelli, A. (2015). Italian and Alpine three-dimensional crustal structure imaged by ambient-noise surface-wave dispersion. *Geochemistry, Geophysics, Geosystems*, *16*(12), 4405–4421. https://doi.org/10.1002/2015GC006176

Molli, G. (2008). Northern Apennine–Corsica orogenic system: An updated overview. *Geological Society, London, Special Publications*, *298*(1), 413–442. https://doi.org/10.1144/SP298.19

Molli, G., Crispini, L., Malusà, M. G., Mosca, P., Piana, F., & Federico, L. (2010). Geology of the Western Alps-Northern Apennine junction area: A regional review. *Journal of the Virtual Explorer*, *36*, 1–49. https://doi.org/10.3809/jvirtex.2010.00215

Mostardini, F., & Merlini, S. (1986). Appennino centro-meridionale: Sesioni geologiche e proposta di modello strutturale. *Memorie della Societa Geologica Italiana*, *35*, 177–202.

Noguera, A. M., & Rea, G. (2000). Deep structure of the Campanian–Lucanian arc (southern Apennine, Italy). *Tectonophysics*, *324*(4), 239–265. https://doi.org/10.1016/S0040-1951(00)00137-2

Norden, B., & Förster, A. (2006). Thermal conductivity and radiogenic heat production of sedimentary and magmatic rocks in the Northeast German Basin. *AAPG Bulletin*, *90*(6), 939–962. https://doi.org/10.1306/01250605100

Pamić, J., Balen, D., & Herak, M. (2002). Origin and geodynamic evolution of Late Paleogene magmatic associations along the Periadriatic-Sava-Vardar magmatic belt. *Geodinamica Acta*, *15*(4), 209–231. https://doi.org/10.1080/09853111.2002.10510755

Pamić, J., Gušić, I., & Jelaska, V. (1998). Geodynamic evolution of the Central Dinarides. *Tectonophysics*, *297*(1), 251–268. https://doi.org/10.1016/S0040-1951(98)00171-1

Pandeli, E., Principi, G., Bortolotti, V., Benvenuti, M., Fazzuoli, M., Dini, A., et al. (2013). The Elba island: An intriguing geological puzzle in the northern Tyrrhenian Sea. In *ISPRA and Soc. Geol. It., Geol. Field Trips, 5(2.1)*.

Patacca, E., Sartori, R., & Scandone, P. (1990). Tyrrhenian Basin and Apenninic arcs: Kinematic relations since late Tortonian times. *Memorie della Societa Geologica Italiana*, *45*, 425–451.

Patacca, E., & Scandone, P. (2001). Late thrust propagation and sedimentary response in the thrust-belt—Foredeep system of the southern Apennines (Pliocene-Pleistocene). In G. B. Vai & I. P. Martini (Eds.), *Anatomy of an orogen: The Apennines and adjacent Mediterranean basins* (pp. 401–440). Springer Netherlands. https://doi.org/10.1007/978-94-015-9829-3_23

Patacca, E., & Scandone, P. (2007). Geological interpretation of the CROP-04 seismic line (Southern Apennines, Italy). *Bollettino-Societa Geologica Italiana*, *7*, 297–315.

Pauselli, C., Barchi, M. R., Federico, C., Magnani, M. B., & Minelli, G. (2006). The crustal structure of the Northern Apennines (Central Italy): An insight by the CROP03 seismic line. *American Journal of Science*, *306*(6), 428–450. https://doi.org/10.2475/06.2006.02

Pauselli, C., Gola, G., Mancinelli, P., Trumpy, E., Saccone, M., Manzella, A., & Ranalli, G. (2019). A new surface heat flow map of the Northern Apennines between latitudes 42.5 and 44.5 N. *Geothermics*, *81*, 39–52. https://doi.org/10.1016/j.geothermics.2019.04.002

Peccerillo, A. (2005). *Plio-quaternary volcanism in Italy: Petrology, geochemistry, geodynamics*. Springer.

Pedreira, D., Afonso, J. C., Pulgar, J. A., Gallastegui, J., Carballo, A., Fernàndez, M., et al. (2015). Geophysical-petrological modeling of the lithosphere beneath the Cantabrian Mountains and the North-Iberian margin: Geodynamic implications. *Lithos*, *230*, 46–68. https://doi.org/10.1016/j.lithos.2015.04.018

Piana Agostinetti, N., & Amato, A. (2009). Moho depth and Vp/Vs ratio in peninsular Italy from teleseismic receiver functions. *Journal of Geophysical Research*, *114*(B6), B06303. https://doi.org/10.1029/2008JB005899

Piana Agostinetti, N., & Faccenna, C. (2018). Deep structure of Northern Apennines subduction orogen (Italy) as revealed by a joint interpretation of passive and active seismic data. *Geophysical Research Letters*, *45*(9), 4017–4024. https://doi.org/10.1029/2018GL077640

Piromallo, C., & Morelli, A. (2003). P wave tomography of the mantle under the Alpine-Mediterranean area. *Journal of Geophysical Research*, *108*(B2), 2065. https://doi.org/10.1029/2002JB001757

Placer, L., Vrabec, M., & Celarc, B. (2010). The bases for understanding of the NW Dinarides and Istria Peninsula tectonics. *Geologija*, *53*(1), 55–86. https://doi.org/10.5474/geologija.2010.005

Plomerová, J., & Babuška, V. (2010). Long memory of mantle lithosphere fabric—European LAB constrained from seismic anisotropy. *Lithos*, *120*(1), 131–143. https://doi.org/10.1016/j.lithos.2010.01.008

Robertson, A., Karamata, S., & Šarić, K. (2009). Overview of ophiolites and related units in the Late Palaeozoic–Early Cenozoic magmatic and tectonic development of Tethys in the northern part of the Balkan region. *Lithos*, *108*(1), 1–36. https://doi.org/10.1016/j.lithos.2008.09.007

Rocchi, S., Westerman, D. S., Dini, A., & Farina, F. (2010). Intrusive sheets and sheeted intrusions at Elba Island, Italy. *Geosphere*, *6*(3), 225–236. https://doi.org/10.1130/GES00551.1

Romagny, A., Jolivet, L., Menant, A., Bessière, E., Maillard, A., Canva, A., et al. (2020). Detailed tectonic reconstructions of the Western Mediterranean region for the last 35 Ma, insights on driving mechanisms. *Bulletin de la Societe Geologique de France*, *191*(1), 37. https://doi.org/10.1051/bsgf/2020040

Rosenbaum, G., Gasparon, M., Lucente, F. P., Peccerillo, A., & Miller, M. S. (2008). Kinematics of slab tear faults during subduction segmentation and implications for Italian magmatism: Kinematics of slab tear faults. *Tectonics*, *27*(2), TC2008. https://doi.org/10.1029/2007TC002143

Rossetti, F., Faccenna, C., Jolivet, L., Funiciello, R., Tecce, F., & Brunet, C. (1999). Syn-versus post-orogenic extension: The case study of Giglio island (northern Tyrrhenian Sea, Italy). *Tectonophysics*, *304*(1), 71–93. https://doi.org/10.1016/S0040-1951(98)00304-7

Royden, L. H. (1993). The tectonic expression slab pull at continental convergent boundaries. *Tectonics*, *12*(2), 303–325. https://doi.org/10.1029/92TC02248

Sandwell, D. T., Müller, R. D., Smith, W. H. F., Garcia, E., & Francis, R. (2014). New global marine gravity model from CryoSat-2 and Jason-1 reveals buried tectonic structure. *Science*, *346*(6205), 65–67. https://doi.org/10.1126/science.1258213

Sani, F., Bonini, M., Montanari, D., Moratti, G., Corti, G., & Ventisette, C. D. (2016). The structural evolution of the Radicondoli–Volterra Basin (southern Tuscany, Italy): Relationships with magmatism and geothermal implications. *Geothermics*, *59*, 38–55. https://doi.org/10.1016/j.geothermics.2015.10.008

Sartori, R., Torelli, L., Zitellini, N., Carrara, G., Magaldi, M., & Mussoni, P. (2004). Crustal features along a W–E Tyrrhenian transect from Sardinia to Campania margins (Central Mediterranean). *Tectonophysics*, *383*(3), 171–192. https://doi.org/10.1016/j.tecto.2004.02.008

Schmid, S. M., Bernoulli, D., Fügenschuh, B., Matenco, L., Schefer, S., Schuster, R., et al. (2008). The Alpine-Carpathian-Dinaridic orogenic system: Correlation and evolution of tectonic units. *Swiss Journal of Geosciences*, *101*(1), 139–183. https://doi.org/10.1007/s00015-008-1247-3

Schmid, S. M., Fügenschuh, B., Kissling, E., & Schuster, R. (2004). Tectonic map and overall architecture of the Alpine orogen. *Eclogae Geologicae Helvetiae*, *97*(1), 93–117. https://doi.org/10.1007/s00015-004-1113-x

Schmid, S. M., Fügenschuh, B., Kounov, A., Matenco, L., Nievergelt, P., Oberhänsli, R., et al. (2020). Tectonic units of the Alpine collision zone between eastern Alps and western Turkey. *Gondwana Research*, *78*, 308–374. https://doi.org/10.1016/j.gr.2019.07.005

Scrocca, D. (2006). Thrust front segmentation induced by differential slab retreat in the Apennines (Italy). *Terra Nova*, *18*(2), 154–161. https://doi.org/10.1111/j.1365-3121.2006.00675.x

Scrocca, D., Doglioni, C., Innocenti, F., Manetti, P., MAZZOTTI, A., Bertelli, L., et al. (2003). *CROP Atlas—seismic reflection profiles of the Italian crust*. Ist. Poligrafico e Zecca dello Stato.

Seghedi, I., & Downes, H. (2011). Geochemistry and tectonic development of Cenozoic magmatism in the Carpathian–Pannonian region. *Gondwana Research*, *20*(4), 655–672. https://doi.org/10.1016/j.gr.2011.06.009

Serri, G., Innocenti, F., & Manetti, P. (1993). Geochemical and petrological evidence of the subduction of delaminated Adriatic continental lithosphere in the genesis of the Neogene-Quaternary magmatism of central Italy. *Tectonophysics*, *223*(1), 117–147. https://doi.org/10.1016/0040-1951(93)90161-C

Smith, W. H. F., & Sandwell, D. T. (1997). Global Sea floor topography from satellite altimetry and ship depth soundings. *Science*, *277*(5334), 1956–1962. https://doi.org/10.1126/science.277.5334.1956

Spakman, W., & Wortel, R. (2004). A tomographic view on western Mediterranean geodynamics. In W. Cavazza, F. Roure, W. Spakman, G. M. Stampfli, & P. A. Ziegler (Eds.), *The TRANSMED Atlas. The Mediterranean region from crust to mantle: Geological and geophysical framework of the Mediterranean and the surrounding areas* (pp. 31–52). Springer. https://doi.org/10.1007/978-3-642-18919-7_2

Stampfli, G. M., & Borel, G. D. (2002). A plate tectonic model for the Paleozoic and Mesozoic constrained by dynamic plate boundaries and restored synthetic oceanic isochrons. *Earth and Planetary Science Letters*, *196*(1), 17–33. https://doi.org/10.1016/S0012-821X(01)00588-X

Stipčević, J., Herak, M., Molinari, I., Dasović, I., Tkalčić, H., & Gosar, A. (2020). Crustal thickness beneath the Dinarides and surrounding areas from receiver functions. *Tectonics*, *39*(3), e2019TC005872. https://doi.org/10.1029/2019TC005872

Šumanovac, F. (2010). Lithosphere structure at the contact of the Adriatic microplate and the Pannonian segment based on the gravity modelling. *Tectonophysics*, *485*(1), 94–106. https://doi.org/10.1016/j.tecto.2009.12.005

Šumanovac, F., & Dudjak, D. (2016). Descending lithosphere slab beneath the Northwest Dinarides from teleseismic tomography. *Journal of Geodynamics*, *102*, 171–184. https://doi.org/10.1016/j.jog.2016.09.007

Šumanovac, F., Hegedűs, E., Orešković, J., Kolar, S., Kovács, A. C., Dudjak, D., & Kovács, I. J. (2016). Passive seismic experiment and receiver functions analysis to determine crustal structure at the contact of the northern Dinarides and southwestern Pannonian Basin. *Geophysical Journal International*, *205*(3), 1420–1436. https://doi.org/10.1093/gji/ggw101

Šumanovac, F., Markušić, S., Engelsfeld, T., Jurković, K., & Orešković, J. (2017). Shallow and deep lithosphere slabs beneath the Dinarides from teleseismic tomography as the result of the Adriatic lithosphere downwelling. *Tectonophysics*, *712–713*, 523–541. https://doi.org/10.1016/j.tecto.2017.06.018

Tari, V. (2002). *Evolution of the northern and western Dinarides: A tectonostratigraphic approach* (Vol. 1, pp. 223–236). Stephan Mueller Special Publication Series. https://doi.org/10.5194/smsps-1-223-2002

Tesauro, M., Kaban, M. K., & Cloetingh, S. A. P. L. (2008). EuCRUST-07: A new reference model for the European crust. *Geophysical Research Letters*, *35*(5), L05313. https://doi.org/10.1029/2007GL032244

Tesauro, M., Kaban, M. K., & Cloetingh, S. A. P. L. (2009). A new thermal and rheological model of the European lithosphere. *Tectonophysics*, *476*(3), 478–495. https://doi.org/10.1016/j.tecto.2009.07.022

Tinterri, R., & Lipparini, L. (2013). Seismo-stratigraphic study of the Plio-Pleistocene foredeep deposits of the Central Adriatic Sea (Italy): Geometry and characteristics of deep-water channels and sediment waves. *Marine and Petroleum Geology*, *42*, 30–49. https://doi.org/10.1016/j.marpetgeo.2012.11.004

Tomljenović, B., Csontos, L., Márton, E., & Márton, P. (2008). Tectonic evolution of the northwestern Internal Dinarides as constrained by structures and rotation of Medvednica Mountains, North Croatia. *Geological Society, London, Special Publications*, *298*(1), 145–167. https://doi.org/10.1144/SP298.8

Trincardi, F., & Zitellini, N. (1987). The rifting of the Tyrrhenian basin. *Geo-Marine Letters*, *7*, 1–6. https://doi.org/10.1007/BF02310459

Trumpy, E., & Manzella, A. (2017). Geothopica and the interactive analysis and visualization of the updated Italian National Geothermal Database. *International Journal of Applied Earth Observation and Geoinformation*, *54*, 28–37. https://doi.org/10.1016/j.jag.2016.09.004

Tunini, L., Jiménez-Munt, I., Fernandez, M., Vergés, J., & Villaseñor, A. (2015). Lithospheric mantle heterogeneities beneath the Zagros mountains and the Iranian plateau: A petrological-geophysical study. *Geophysical Journal International*, *200*(1), 596–614. https://doi.org/10.1093/gji/ggu418

Ustaszewski, K., Kounov, A., Schmid, S. M., Schaltegger, U., Krenn, E., Frank, W., & Fügenschuh, B. (2010). Evolution of the Adria-Europe plate boundary in the northern Dinarides: From continent-continent collision to back-arc extension. *Tectonics*, *29*(6), TC6017. https://doi.org/10.1029/2010TC002668

van Hinsbergen, D. J. J., Maffione, M., Koornneef, L. M. T., & Guilmette, C. (2019). Kinematic and paleomagnetic restoration of the Semail ophiolite (Oman) reveals subduction initiation along an ancient Neotethyan fracture zone. *Earth and Planetary Science Letters*, *518*, 183–196. https://doi.org/10.1016/j.epsl.2019.04.038

van Hinsbergen, D. J. J., Torsvik, T. H., Schmid, S. M., Matenco, L. C., Maffione, M., Vissers, R. L. M., et al. (2020). Orogenic architecture of the Mediterranean region and kinematic reconstruction of its tectonic evolution since the Triassic. *Gondwana Research*, *81*, 79–229. https://doi.org/10.1016/j.gr.2019.07.009

van Unen, M., Matenco, L., Nader, F. H., Darnault, R., Mandic, O., & Demir, V. (2019). Kinematics of foreland-vergent crustal accretion: Inferences from the Dinarides evolution. *Tectonics*, *38*(1), 49–76. https://doi.org/10.1029/2018TC005066

Vezzani, L., Festa, A., & Ghisetti, F. C. (2010). *Geology and tectonic evolution of the central-southern Apennines, Italy*. Geological Society of America. https://doi.org/10.1130/SPE469

Vignaroli, G., Faccenna, C., Jolivet, L., Piromallo, C., & Rossetti, F. (2008). Subduction polarity reversal at the junction between the Western Alps and the northern Apennines, Italy. *Tectonophysics*, *450*(1), 34–50. https://doi.org/10.1016/j.tecto.2007.12.012

Vignaroli, G., Faccenna, C., Rossetti, F., & Jolivet, L. (2009). Insights from the Apennines metamorphic complexes and their bearing on the kinematics evolution of the orogen. *Geological Society, London, Special Publications*, *311*(1), 235–256. https://doi.org/10.1144/SP311.9

Vilà, M., Fernández, M., & Jiménez-Munt, I. (2010). Radiogenic heat production variability of some common lithological groups and its significance to lithospheric thermal modeling. *Tectonophysics*, *490*(3), 152–164. https://doi.org/10.1016/j.tecto.2010.05.003

Wessel, P., & Smith, W. H. F. (1998). New, improved version of generic mapping tools released. *Eos, Transactions American GeophysicalUnion*, *79*(47), 579. https://doi.org/10.1029/98EO00426

Workman, R. K., & Hart, S. R. (2005). Major and trace element composition of the depleted MORB mantle (DMM). *Earth and Planetary Science Letters*, *231*(1), 53–72. https://doi.org/10.1016/j.epsl.2004.12.005

Wrigley, R., Hodgson, N., & Esestime, P. (2015). Petroleum geology and hydrocarbon potential of the Adriatic Basin, offshore Croatia. *Journal of Petroleum Geology*, *38*(3), 301–316. https://doi.org/10.1111/jpg.12612

Zhao, L., Paul, A., Malusà, M. G., Xu, X., Zheng, T., Solarino, S., et al. (2016). Continuity of the Alpine slab unraveled by high-resolution P wave tomography. *Journal of Geophysical Research: Solid Earth*, *121*(12), 8720–8737. https://doi.org/10.1002/2016JB013310

Zhu, H., Bozdağ, E., & Tromp, J. (2015). Seismic structure of the European upper mantle based on adjoint tomography. *Geophysical Journal International*, *201*(1), 18–52. https://doi.org/10.1093/gji/ggu492